

USE OF THE FLUORIDE VOLATILITY PROCESS TO EXTRACT
TECHNETIUM FROM TRANSMUTED
SPENT NUCLEAR FUEL

A Thesis

Presented in Partial Fulfillment of the Requirements for
the Degree Master of Science in the
Graduate School of The Ohio State University

By

Benjamin James Milliron, B.S.

The Ohio State University
2002

Master's Examination Committee:

Dr. Richard S. Denning, Adviser

Dr. Audeen Fentiman

Approved by

Adviser

Nuclear Engineering Graduate Program

ABSTRACT

The US Department of Energy (DOE) is currently developing the technology needed to partition and transmute spent nuclear fuel to reduce the long-term hazards of geologic disposal. The Advanced Fuel Cycles Initiative (AFCI) project will require a variety of separations processes, including the separation of transuranic elements and certain fission products. Of the fission products, technetium and iodine are to be transmuted. Within a geologic repository, the chemistry of technetium and iodine affords them high mobility in a groundwater system. Because of the long lifetimes of Tc99 and I129 and their relative mobility, it is desirable to remove these elements from the waste stream and transmute them with the transuranic elements. The objective of this study is to identify means to chemically separate technetium from other metals in the waste stream of pyrochemically processed fuel.

The baseline fuel for post-transmutation processing is a TRU-Zircaloy metal alloy fuel. Pyrochemical processing is preferred over aqueous processing for metal fuels for economic factors, and is used in the first stages of the post-transmutation processing scheme. In the pyrochemical process, the Tc remains with the cladding, metal matrix and noble metal fission products. A separation process is required to recover Tc from these metal residuals prior to their disposal in the metal waste form. This process needs to be

compatible with the upstream pyrochemical steps and the existing waste forms. Fluoride volatilization may prove viable in this respect.

The fluoride volatility process has been widely researched as a method for the separation of metals for many years. The procedure involves introducing a highly reactive fluorinating agent, usually hydrogen fluoride (HF) or by fluorine gas (F₂), to the metal. HF reacts with the metals, forming volatile metallic fluorides. This increased volatility is exploited to achieve separation with standard distillation/absorption techniques.

FACTSage® (7), a chemical equilibrium code, is used to model the fluoride volatility process in this thesis. This code uses thermochemical data of species to predict the final equilibrium composition of the chemical system. The scarcity of Tc results in a relative lack of literature regarding the compounds and chemistry of Tc. Thus, in order to perform the required calculations, some thermochemical data for the technetium fluorides had to be modeled. Predicted values of $\Delta H_o^f = -1200$ kJ/mol for TcF₅ and $\Delta H_o^f = -1210$ kJ/mol for TcF₆ are in agreement with other available predictions. Modeling results indicate that Tc can be quantitatively volatilized via reaction with F₂ gas. TcF₆ is formed along with other volatile hexafluorides. These volatile compounds comprise only 1% of the original mass of metal. The TcF₆ can be isolated from the other volatile compounds and reduced by other industrially accepted methods. The metallic Tc can then be transmuted. The next step in demonstrating the feasibility of the proposed approach to separating Tc by fluorination would be to demonstrate the formation of the expected chemical species through experimentation. A surrogate experiment that has significant cost and safety advantages is suggested and modeled in this thesis.

Dedicated to James LaBrie, Keith Maupin, and Peter Tosh

ACKNOWLEDGMENTS

I wish to thank my adviser, Dr. Richard Denning, for his patience, support, understanding, and unwavering enthusiasm throughout this project.

I thank Dr. Diane Graziano and all of her associates at Argonne National Laboratory for their invaluable guidance and review of this thesis.

I thank Dr. Philip Spencer for his attentive help with the FACTSage® software.

This thesis is the final product of the Advanced Accelerator Applications Fellowship that I was awarded from the US Department of Energy. I wish to thank all those involved with the establishment of this fellowship, without which none of the research presented would have been possible.

VITA

August 9, 1977 Born – Kalamazoo, Michigan
2000 B.S. Chemical Engineering, The University
of Toledo
2001 – present Fellowship Research, The Ohio State
University

FIELDS OF STUDY

Major Field: Nuclear Engineering

Undergraduate Field: Chemical Engineering

TABLE OF CONTENTS

	<u>Page</u>
Abstract	ii
Acknowledgments.....	v
Vita	vi
Fields Of Study	vii
1 - Introduction	1
2 - Background.....	4
2.1 In depth review of the AFCI project	4
2.2 AfcI Separations Overview	6
2.2.1 The UREX Process	9
2.2.2 The Pyro-A Process	11
2.2.3 The Pyro-B Process.....	15
3 - Fluoride Volatility Process	18
3.1 Introduction.....	18
3.2 Reasons For Investigating The Fluoride Volatility Process	18
3.3 Modeling.....	21
4 - Estimating Missing Thermodynamic Data	24
4.1 Background.....	24
4.2 Literature Values.....	24
4.3 Approximating Heat Of Formation Data	26
5 - Equilibrium Modeling Results	37
5.1 Input For Modeling.....	37
5.2 Explanation of results	38
5.3 Results of HF reaction	38
5.4 Results of F ₂ reaction.....	41
5.5 Isolation of TcF ₆	45
5.6 Final Tc Waste Form	47
6 - Conclusions And Suggestions For Further Work.....	49
6.1 Review	49
6.2 Suggestions For Further Work.....	50

Appendices

A - Theory For Predicting Chemical Equilibrium	54
B - Suggested Surrogate Experiment	64
B.1 Background	64
B.2 Experimental Setup	66
B.3 Experimental Uncertainties	67
C - Modeling Of The Surrogate Experiment	69
C.1 Feed composition	69
C.2 FACTSage® Modeling Input and Results	74
C.3 Review of Surrogate Experiment Modeling	86

LIST OF TABLES

Table

Table 2.1: Composition of US spent nuclear fuel (14)	5
Table 3.1: Predicted output of transmutation scheme to be considered for a fluorination model (Data from ANL)	20
Table 3.2: List of metal-fluorides and their boiling points (17).....	23
Table 4.1: List of physical and thermodynamic data for TcF ₅ and TcF ₆ (4), (11).....	25
Table 4.2: Enthalpies of formation for known difluorides.....	28
Table 5.1: Major gaseous products from the reaction of metals listed in Table 3.1 with Excess F ₂ , T = 60 – 100C	44
Table 5.2: Vapor pressures of selected compounds at 80 C	46
Table C.1: Compositions of SS-316/Zircaloy-2 mixture vs. theoretical feed for fluorination scheme.....	73
Table C.2: Pressure and major gaseous products from reaction of varying amounts of F ₂ gas with 50.3% SS-316 and 49.7% Zircaloy-2, at 100 C.....	76
Table C.3: Major gaseous products from reaction of 50.3% SS-316 & 49.7% Zircaloy-2 with 14.6g F ₂ (100C).....	79
Table C.4: Gaseous products from reaction of F ₂ gas with SS-316/Zircaloy2, with varying amounts of initial air/F ₂	84
Table C.5: Gaseous products from reaction of F ₂ gas with SS-316/Zircaloy2, with varying amounts of initial air (Constant F ₂)	85

LIST OF FIGURES

Figure

Figure 2.1:	Overview of the main separations schemes of the AFCI Project	8
Figure 2.2:	Schematic of the UREX process in the AFCI project.....	10
Figure 2.3:	A schematic of the Pyro-A process.....	12
Figure 2.4:	The electrorefining operation.....	14
Figure 2.5:	A schematic of the Pyro-B process.....	16
Figure 4.1:	The Pettifor single string rearrangement of the periodic table in the sequence of the Mendeleev number.....	27
Figure 4.2:	Enthalpy of formation vs. Mendeleev number for known difluorides....	30
Figure 4.3:	Enthalpy of formation vs. Mendeleev number for known trifluorides ...	31
Figure 4.4:	Enthalpy of formation vs. Mendeleev number for known tetrafluorides	32
Figure 4.5:	Enthalpy of formation vs. Mendeleev number for known pentafluorides.....	33
Figure 4.6:	Enthalpy of formation vs. Mendeleev number for known hexafluorides	35
Figure 5.1:	Major gaseous products from reaction of metals listed in Table 3.1 with Excess F ₂ , Temp = 20 – 100 C (F ₂ gas omitted).....	39
Figure 5.2:	Major gaseous products from reaction of metals listed in Table 3.1 with Excess HF, Temp = 20 – 500 C	40
Figure 5.3:	Major gaseous products from reaction of metals listed in Table 3.1 with Excess F ₂ , Temp = 20 – 100 C (F ₂ gas omitted).....	42
Figure 5.4:	Major gaseous products from reaction of metals listed in Table 3.1 with Excess F ₂ , Temp = 20 – 500 C (F ₂ gas omitted).....	43

Figure B.1:	Major gaseous products from F ₂ reaction with metals in Table 3.1	65
Figure C.1:	Compositions of SS-316/Zircaloy-2 mixture vs. theoretical feed for fluorination scheme.....	70
Figure C.2:	Major elements of SS-316/Zircaloy-2 mixture vs. theoretical feed for fluorination scheme.....	71
Figure C.3:	Products from reaction of varying amounts of F ₂ gas with 50.3% SS-316 and 49.7% Zircaloy-2, at 100 C	75
Figure C.4:	Major gaseous products from reaction of 50.3% SS-316 & 49.7% Zircaloy-2 with 14.6g F ₂ (20 - 100C)	78
Figure C.5:	Major gaseous products from reaction of 50.3% SS-316 & 49.7% Zircaloy-2 with 14.6g F ₂ (20 – 100 C).....	80
Figure C.6:	Gaseous products from reaction of F ₂ gas with SS-316/Zircaloy2, with varying amounts of initial air/F ₂ mix	82
Figure C.7:	Gaseous products from reaction of F ₂ gas with SS-316/Zircaloy2, with varying amounts of initial air (constant F ₂)	83

CHAPTER 1

INTRODUCTION

The US government recently approved the Yucca Mountain site as a geologic repository for the nation's spent nuclear fuel. This action has aroused serious public and political concern over the safety issues associated with a potential repository leak which could pose a health risk to the local population. One way to ease this concern would be to remove the most hazardous compounds from the fuel prior to burial. With this in mind, the US Department of Energy (DOE) proposed the Accelerator Transmutation of Waste (ATW) project, which is now called the Advanced Fuel Cycles Initiative (AFCI) Project (1). To make burial safer, the project aims to remove and process different elements of the spent fuel for either low-level storage or transmutation of specific elements into safer, less hazardous species. Should the transmutation of waste be fully realized, the only elements to be buried at the Yucca Mountain site would be fission products (FPs). Currently, technetium and iodine are to be transmuted while the transuranic elements (TRUs) are to be fissioned. The process of fissioning the TRUs will generate quantities of additional technetium along with many other elements as FPs in

metallic form. The technetium from the transmuted TRUs must be removed and recycled back into the transmutation scheme before the FPs can be prepared for burial. The fluoride volatility process has been suggested as a method for removing the Tc from post-transmutation AFCI fuel. This process has been widely used for decades in the conversion of oxide to hexafluoride for uranium enrichment. A fluoride volatility process involves introducing a highly reactive fluorinating agent to the chopped metal fuel (or any composite of materials) to form volatile metallic fluorides. The increased volatility is exploited to achieve separation with standard distillation/absorption techniques. This thesis is a study of the feasibility of using this process as a method of separating Tc from post-transmutation AFCI fuel.

The ideal way to determine feasibility of this process would undoubtedly be to determine the composition of the post-transmutation AFCI fuel, design and create an identical mock-up, and perform fluorination experiments in a laboratory. However, until the feasibility of the approach has been established, the expense of this approach can't be warranted. In addition, the prototypic materials are highly radioactive. An accurate mock-up of TRUs that have undergone a transmutation scheme would contain many highly radioactive elements. The use of Tc alone presents a radiation risk, since there are no stable isotopes of Tc. If non-radioactive elements were used, the mock-up would still contain many highly toxic compounds, including (but not limited to) the fluorides CrF_4 , ZrF_4 , MoF_6 , SiF_4 , NiF_2 and MnF_3 . In addition, the assembly of the many required rare-earth elements and other products would present an enormous expense.

To avoid personnel safety risks and high costs, a computer simulation is used to model the fluorination process. There are many commercially available chemical

reaction codes available for such tasks. FACTSage® was chosen as a modeling tool for this work (6). This software predicts the chemical equilibrium composition of a user-defined system. In this case, FACTSage® is used to determine the proper fluorinating agent, the amount of the fluorinating agent, the volatility of the metal fluorides and whether or not the technetium fluoride can be condensed.

CHAPTER 2

BACKGROUND

2.1 In depth review of the AFCI project

Spent light-water nuclear reactor fuel consists of a variety of different metallic oxides in a Zr-based cladding. Many of these metals are toxic and/or radioactive and some raise proliferation concerns. The composition of commercial spent fuel is shown in Table 2.1.

Element	Weight Percent
Uranium	95.6%
Stable/Short-lived fission products	3.0%
Plutonium	0.9%
Cesium/Strontium	0.3%
Minor Actinides (<i>Np, Am, Cm</i>)	0.1%
Iodine, Technetium	0.1%

Table 2.1: Composition of US spent light-water nuclear reactor fuel (excluding cladding and hardware) (14)

The elements to be removed from spent nuclear fuel include uranium, TRUs, Tc, and I. Uranium makes up 95.6% of spent fuel and, if removed, could be stored in a low-level waste facility, eliminating a large fraction of the volume needed for geologic repository. TRUs are to be removed because of their long lifetimes and radioactivity level and their potential value in providing additional fission energy. The Pu is also a serious public concern because of its potential use in nuclear weapons production. The chemistry of Tc and I affords them high mobility if released from the waste system in a groundwater system. Studies have shown that, on a geologic time scale (100,000 years),

dose rates around a geologic burial site would be highest from ^{237}Np , ^{99}Tc , and ^{129}I (8).

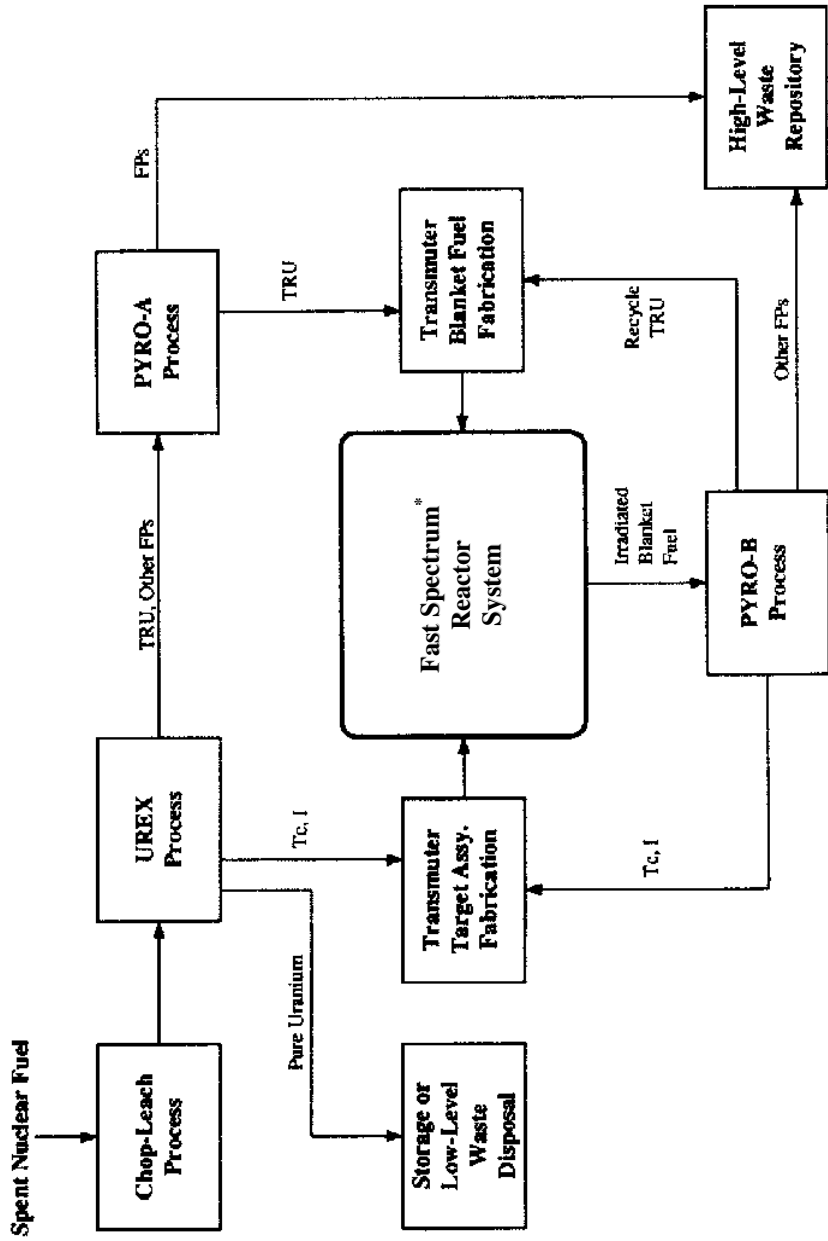
Once the elements of spent fuel mentioned here are removed, less than 4% of the original mass of spent fuel will remain to be buried in a geologic repository.

A brief overview of the original ATW partitioning roadmap, labeled here as AFCI partitioning processes is presented here for a better understanding of the entire system and a feel for exactly where the type of Tc removal investigated here fits in the overall scheme of the AFCI project.

2.2 AFCI Separations Overview

The AFCI program encompasses separation processes of both existing fuel and transmuted fuel. In all of these steps, a minimum of 99.9% of the TRUs and 95% of Tc/I must be removed from the fuel. One option for treating LWR fuel is the UREX process. UREX separates U, TRUs/FPs, and Tc/I from raw commercial spent fuel. Uranium will be placed in a low-level repository, and the Tc and I will be prepared for transmutation. The second scheme (Pyro-A) will separate the TRUs from the FPs and fashion those TRUs into transmuter blanket assemblies. The FPs will be stabilized and sent to the geologic repository. The transmutation process itself will probably be performed in a fast-spectrum reactor. Just as in a commercial nuclear power plant, the fissions of the TRUs produce FPs, including Tc and I which must be removed and recycled back into

the transmuter. The third separations scheme (Pyro-B) will isolate TRUs, Tc, I and FPs from the irradiated TRU transmuter blankets. The newly formed FPs will be buried with those from the commercial spent fuel in the geologic repository. A schematic of the original partitioning scheme for the original ATW scheme (again, labeled as AFCI) is presented in Figure 2.1.



* This process flow diagram was developed with the assumption that transmutation would occur in a subcritical assembly driven by an accelerator. In the current program plan (AFCI), the accelerator driven assembly would be replaced by a fast spectrum reactor system. Other changes could also be made in this flow sheet

Figure 2.1: Overview of the main separations schemes of the AFCI project (8)

2.2.1 The UREX Process

The uranium extraction process (UREX) is similar to the well-known plutonium/uranium extraction process called PUREX that has been used for decades. PUREX is a solvent-based process that separates U and Pu from spent fuel. The UREX process is different in that the Pu is not a separate output stream and is removed along with the FPs and most of the TRUs. The uranium that would be isolated in the UREX process would be ~0.8% fissile ^{235}U (8), or about the same as natural uranium. These two aspects of the process eliminate many of the proliferation concerns that would arise should a process like this be implemented in the US. A schematic of the UREX process is shown in Figure 2.2.

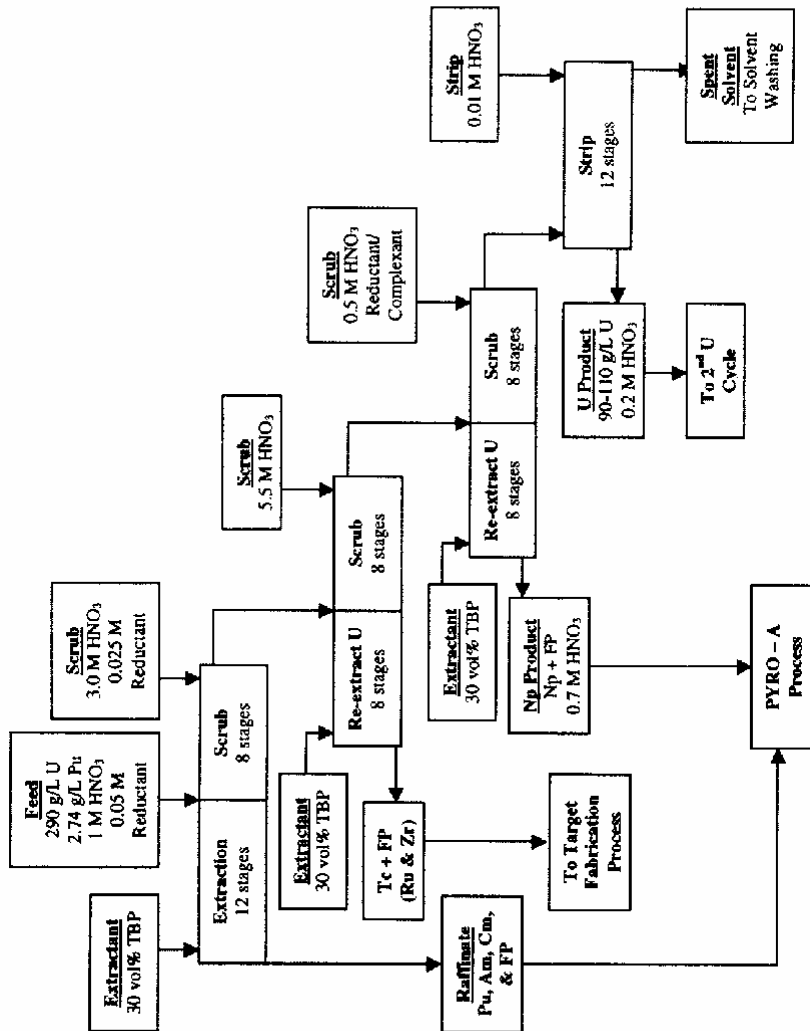


Figure 2.2: Schematic of the UREX process in the AFCI project (8)

Prior to the solvent introduction, the spent fuel is dissolved in nitric acid and sparged with air and NO. This removes the required 95% of the iodine. The I is then sent to transmutation target fabrication. The U extraction is performed by multiple series of centrifugal contactor trains with multiple solvent extraction steps. TRUs (except Np) are removed early and sent to the Pyro-A process along with some accompanying FPs. The Tc is stripped in the second solvent extraction and sent to transmutation target fabrication.

2.2.2 The Pyro-A Process

The TRUs (including Pu) and FPs from the UREX process (which are still dissolved in nitric acid) are sent to the Pyro-A process. The process schematic is shown in Figure 2.3. The nitric acid TRU/FPs solution is heated in a process called thermal denitration, which heats the solution to help remove the nitrogen. After denitration, oxygen must be removed, which is accomplished by reacting the TRUs and FPs with Li metal, which combines with the oxygen leaving the TRUs and FPs behind as pure metals. The TRUs are used in recycled fuel, but must first be isolated from the FPs which would poison the neutron production scheme.

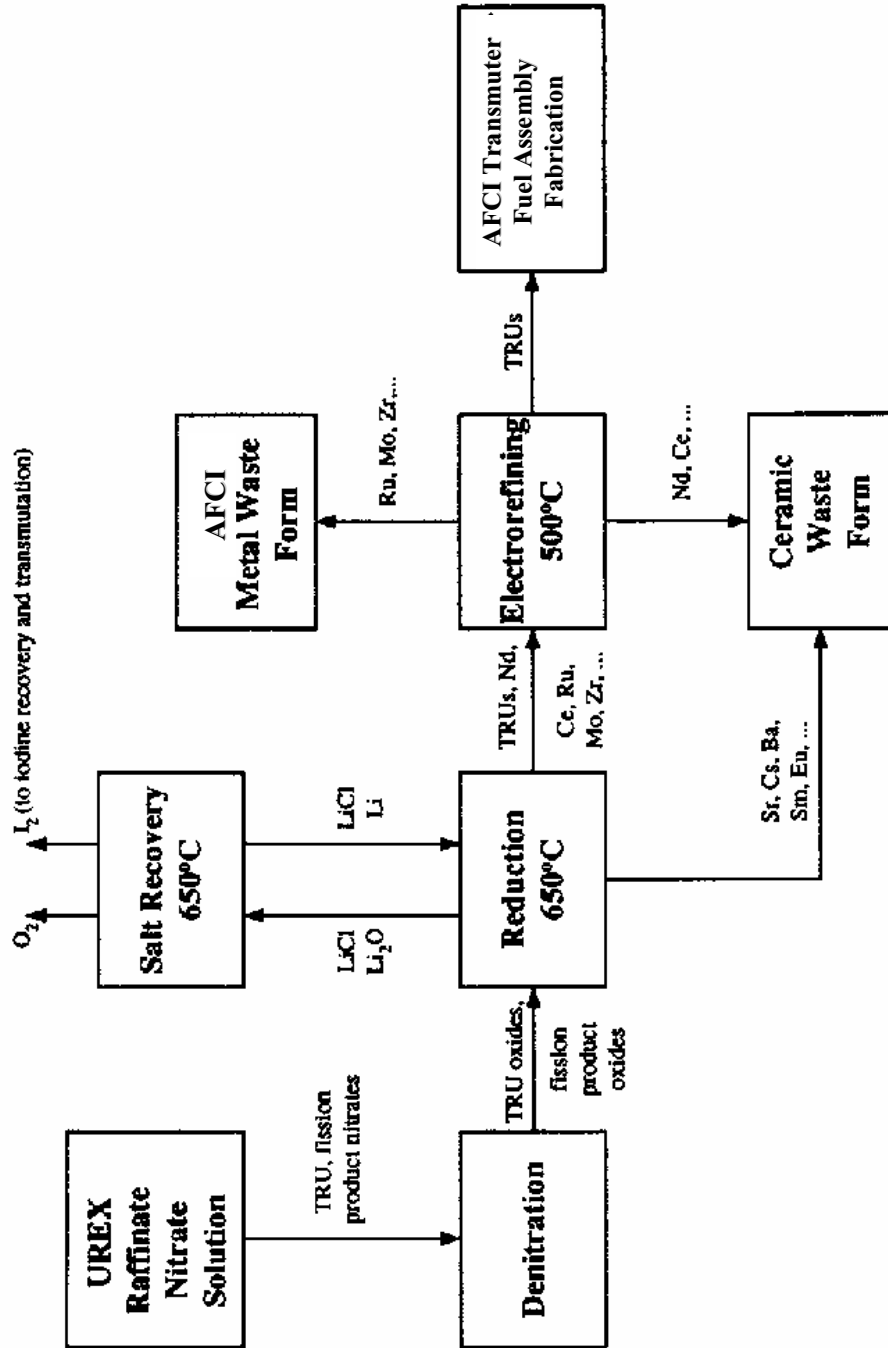


Figure 2.3: A schematic of the Pyro-A process (8)

To separate the TRUs, a process called electrorefining is used. This process is shown in Figure 2.4. In this process, the metals are placed in a steel mesh basket that is submerged into molten salt. A solid SS rod is placed in the pool near the basket. A voltage is applied between the basket and the rod, the basket becoming the anode and the SS rod the cathode. At the anode, electrons are stripped from the TRUs, causing them to enter the salt phase with a positive charge (ions). The current between the anode and the cathode drives the TRU ions towards the negatively charged cathode, where the electrons return to the TRUs, which become metallic again. The metallic TRUs immediately deposit themselves on the cathode and a large growth of dendritic deposits soon forms. (The process is analogous to a car battery with its bluish-white powdery deposits on the positive cathode.) The TRUs are periodically removed from the cathode and sent to the transmutation process. The conditions of the electrorefiner can be regulated to selectively deposit the TRUs, while the FPs are left behind. Some of the FPs will be dissolved in the salt, while others are left behind in the anode basket in their metallic form. The FPs in the salt are treated, mixed with small bits of glass and zeolite, melted, and then cooled to form a glassy solid that is the final waste form. The metallic FPs left in the anode basket are melted with other metals to form another final waste form. These two waste forms, dubbed ceramic and metallic, respectively, are treated as high-level radioactive waste to be buried in a geologic repository.

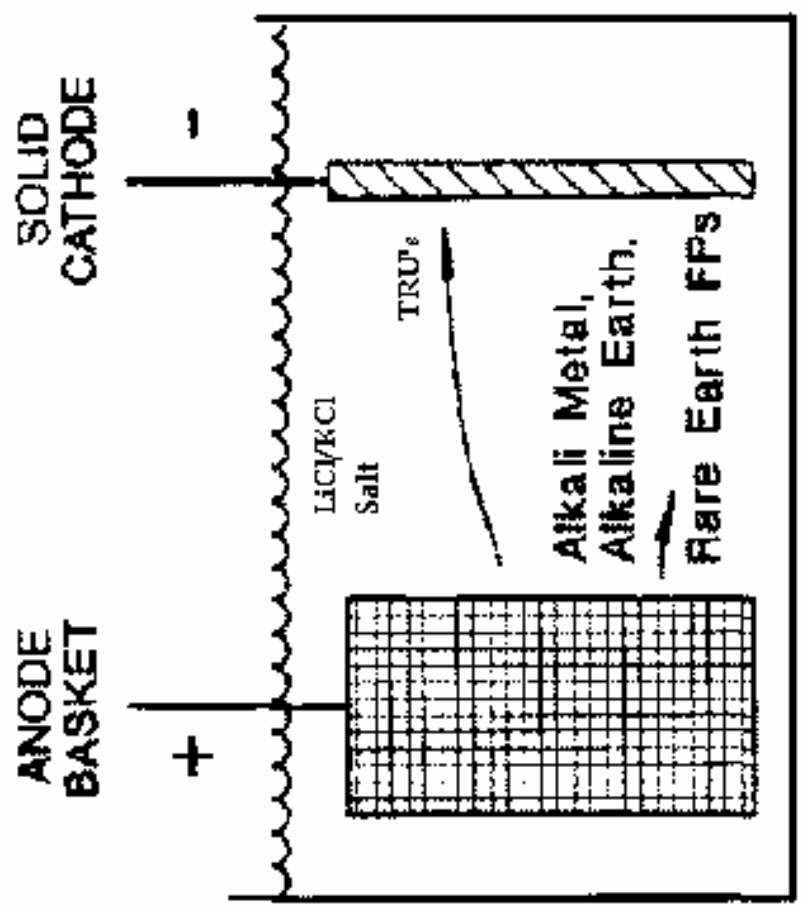


Figure 2.4: The electrorefining operation (8)

2.2.3 The Pyro-B Process

Tc and I are transmuted by heavy bombardment of neutrons. To produce the high neutron flux required for transmutation, the TRUs from the Pyro-A processed are used as blankets in the transmutation scheme. The concept of target assemblies was developed for the Accelerator Transmutation of Waste (ATW) accelerator driven subcritical reactor system (1), (15). With the transition in approach from accelerator-driven to fast spectrum reactor, some aspects of the fuel cycle system can be expected to change. Once the transmuted TRUs emerge from the transmutation scheme, they will be subjected to the Pyro-B process. A schematic is shown in Figure 2.5.

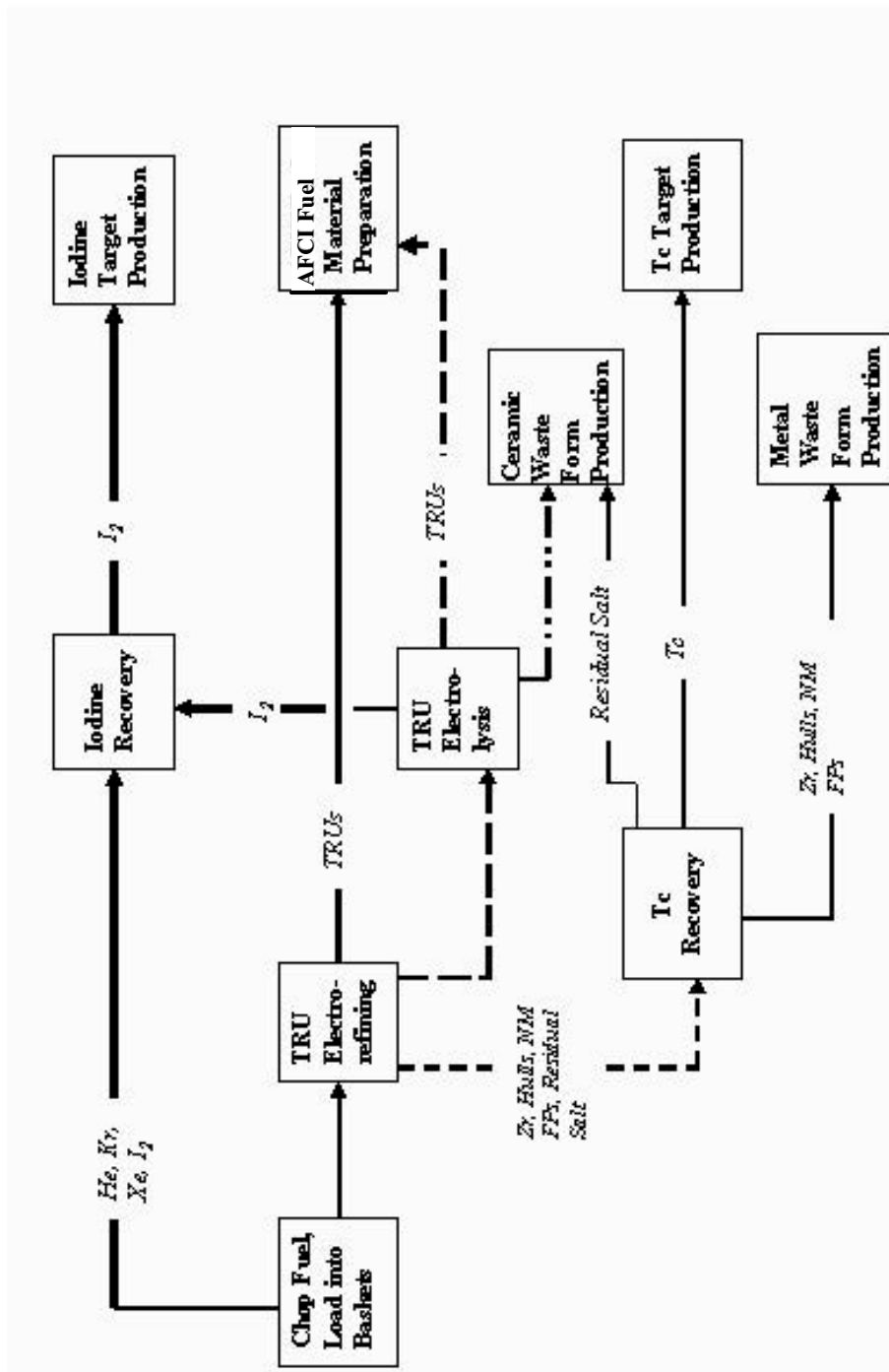


Figure 2.5: A schematic of the Pyro-B process

The process is similar to the initial processes: the fuel is chopped to remove 95% of the iodine and nearly all of the trapped gases, and then treated in an electrorefiner where the bulk of the separation takes place. 99.9% of the TRUs are collected at the cathode and recycled to the transmuter assemblies. The FPs that dissolve in the salt are formed into a similar ceramic waste as in the Pyro-A process. The FPs in the anode basket will contain technetium that was created in the transmutation process, which will have to be removed. The method for doing this has not been defined. It might seem logical to use the same technetium removal method as used in the UREX process. This cannot be done, as it would involve dissolving the FPs in nitric acid and subsequent reduction of the metals. This reduction step is very expensive, and a non-aqueous method is desirable. One method suggested is the fluoride volatility process that is the subject of this thesis. Another method is electrorefining, similar to methods described in the Pyro-A and Pyro-B processes (16). A chloride volatility process has been suggested as well (8). Once the Tc has been recovered (from whatever method employed), it is recycled back into the transmutation scheme along with the recovered TRUs.

CHAPTER 3

FLUORIDE VOLATILITY PROCESS

3.1 Introduction

The fluoride volatility process is typically used in preparing uranium for enrichment. The idea is to react the metals with a compound that contains fluorine, creating metal fluorides. Some of the metal fluorides will become volatile, most notably the hexafluorides. The increased volatility can be exploited to achieve a separation.

3.2 Reasons for investigating the fluoride volatility process

A computer model will be used to simulate fluorination of FPs from the transmuted AFCI fuel¹ along with the fuel cladding. As mentioned in Chapter 2, the

¹ Throughout the rest of this thesis, the term “AFCI fuel” will be used to describe the metal residue from the electrorefiner in the Pyro-B process (Figure 2.5).

TRUs and certain other transmutation products are separated earlier in the Pyro-B process. Table 3.1 lists all of the elements that need to be considered in the model. The list is provided by ANL and derived by ORIGEN simulations, a standardized code that predicts isotope generation analysis in a nuclear reactor. A variety of FPs are listed, along with the cladding material (SS & matrix Zr – Zr, Fe, Cr, Mn, Ni, Co). It is important to remember that these elements are in metallic form.

Element	Metal Residue from Electrorefiner in Pyro-B Process
Zr	1.62866
Fe	0.9806
Cr	0.1325
Mo	0.04215
Ru	0.022535
Pd	0.01687
Rh	0.007611
Tc	0.006079
Ni	0.005734
Te	0.004497
Ag	0.001797
Cd	0.001231
Mn	0.001051
Sn	0.000917
Sb	0.000302
Se	0.000239
In	0.00009
Co	0.000012
Ge	0.000007
Nb	0.000006

Table 3.1: Predicted output of transmutation scheme to be considered for a fluorination model (Data from ANL)

Fluorides of the metals in Table 3.1 are listed in Table 3.2. This table shows that the Se, Te, Mo and Tc hexafluorides boil at the lowest temperatures, respectively, and thus will be the most volatile. Note that other fluorides listed are not hexafluorides and subsequently are not as volatile. This implies that, so long as the hexafluorides are generated, only Mo and Tc will volatilize appreciably and can be separated.

3.3 Modeling

One of the major concerns in chemical modeling is choosing between kinetic and equilibrium methods. The thesis will use equilibrium modeling because the Tc recovery process will probably be a batch process where equilibrium can be approached. In addition, the data required for equilibrium calculations is usually readily available, while kinetic data are rarer. Fluorine-metal reaction kinetic data of the kind needed for this type of system are especially rare, making kinetic modeling much more difficult and unreliable.

The fluoride volatility process is modeled with FACTSage®, a chemical equilibrium computer code. Reactants are defined and equilibrium is determined from the governing laws of chemical thermodynamics. The method used is discussed in Appendix A. FACTSage® requires heat of formation, heat of transformation, melting and boiling point, density, and heat capacity data for every reactant and possible product.

Although FACTSage® comes with an extensive database, some of the required values were not included and must be determined either through research or prediction. Most notably, the values for technetium fluorides are non-existent and must be determined. Methods for estimating missing values are discussed in Chapter 4.

Fluoride	Boiling Point (K)
SeF ₆	226
TeF ₆	234
MoF ₆	307
TcF ₆	328
SeF ₄	374
SbF ₅	414
TeF ₄	467
TcF ₅	480
MoF ₅	486
[RuF ₅] ₆	500
SbF ₃	618
SnF ₄	978
SnF ₂	1123
ZrF ₂	1185
NiF ₂	1273
AgF	1423
CrF ₂	1573
CoF ₂	1673
CdF ₂	2021
MnF ₂	2093

Table 3.2: List of metal-fluorides and their boiling points (17)

CHAPTER 4

ESTIMATING MISSING THERMODYNAMIC DATA

4.1 Background

With any simulation, the output is only as good as the input. Technetium fluoride data are particularly important to make the equilibrium model results valid. FACTSage® has no data for TcF_6 or TcF_5 , both of which are known to exist. Required data for these two compounds must be found in the literature or estimated.

4.2 Literature values

TcF_5 and TcF_6 are the only known metal fluorides studied. Metal alloying is ignored. Oxyfluorides are ignored also, since the Pyro-B process is designed to be oxygen free. It is important to note that there may be some unknown metal fluoride compounds in the system that FACTSage® cannot account for. Values for the boiling

point, melting point, heat of transformation and low temperature heat capacity data were found via a literature search. Note that TcF_6 exists as a solid in two crystalline forms, (designated as s1 and s2) with the transition occurring at 268K.

Species	mp (K)	bp (K)	ΔH_{trans} (kJ/mol)	Temp. of Trans. (K)	S (J/mol/K)
TcF_5 (s)	323.15	-	-	-	205 ^[4]
TcF_5 (l)	-	-	1144 ^[4]	323 ^[4]	-
TcF_5 (g)	-	-	-	-	-
TcF_6 (s1)	310.50	-	-	-	351.283 ^[111]
TcF_6 (s2)	-	-	8025 ^[111]	268.335 ^[111]	-
TcF_6 (l)	-	328.45	4619 ^[111]	311.14 ^[111]	-
TcF_6 (g)	-	-	2985 ^[111]	328.3 ^[111]	-

Table 4.1: List of physical and thermodynamic data for TcF_5 and TcF_6 (4), (11)

Glassner tabulated values for ΔC_p , ΔS_o^f , and ΔH_o^f that were either known or estimated by “analogy with compounds of neighboring elements” (4). Glassner’s data were assembled in 1957, and much more data have been gathered since then, which should allow for a

more reliable estimation method, which will be presented in Section 4.3 along with values given by the Glassner tables.

4.3 Approximating heat of formation data

The most important data needed for equilibrium modeling is the heat of formation (ΔH_o^f) of the compounds. Since FACTSage® does not have the data, it must be estimated. The method employed to approximate these data is relatively new and has been described as the Pettifor method. Pettifor organized the periodic table into a single continuum of elements based on what he called the “Mendeleyev number” (13). The number assigned to each element is based on chemical similarities between elements and was originally used for predicting thermochemical values of binary alloys. The table, organized with a string running along the sequential Mendeleyev numbers, is shown in Figure 4.1.

The image shows a single string rearrangement of the periodic table. Elements are listed in a single vertical column, with their atomic numbers and group labels. The elements are arranged in a zig-zag pattern across the table's width, starting from Hydrogen (H) at the top and ending with Francium (Fr) at the bottom. The groups are labeled as follows: O IA, IIIA IIIA IVA VA VIA VIIA VIIIA VIIIIB VIIIIC IB, IIB IIIIB IVB VB VIB VIIB VIIIB, and 103 H. The elements are: H (1), He (2), Li (3), Be (4), B (5), C (6), N (7), O (8), F (9), Ne (10), Na (11), Mg (12), Al (13), Si (14), P (15), S (16), Cl (17), Ar (18), K (19), Ca (20), Sc (21), Ti (22), V (23), Cr (24), Mn (25), Fe (26), Co (27), Ni (28), Cu (29), Zn (30), Ga (31), Ge (32), As (33), Se (34), Br (35), Kr (36), Rb (37), Sr (38), Y (39), Zr (40), Nb (41), Mo (42), Tc (43), Ru (44), Rh (45), Pd (46), Ag (47), Cd (48), In (49), Sn (50), Sb (51), Te (52), Xe (53), I (54), Ba (55), La (56), Ce (57), Pr (58), Nd (59), Pm (60), Sm (61), Eu (62), Gd (63), Tb (64), Dy (65), Ho (66), Er (67), Tm (68), Yb (69), Lu (70), Hf (71), Ta (72), W (73), Re (74), Os (75), Ir (76), Pt (77), Au (78), Hg (79), Tl (80), Pb (81), Bi (82), Po (83), At (84), Rn (86), Fr (87), Ra (88), Ac (89), Th (90), Pa (91), U (92), Np (93), Pu (94), Am (95), Cm (96), Bk (97), Cf (98), Es (99), Fm (100), Md (101), No (102), and Lr (103).

Figure 4.1: The Pettifor single string rearrangement of the periodic table in the sequence of the Mendeleev number.

Figure courtesy of Philip Spencer (13)

A plot of the free energy of formation of metal halides of similar structure versus Mendeleev number shows trends in the data that can be used to estimate ΔH_o^f values. A table for solid difluorides is shown in Table 4.2.

Compound	Mendeleev Number	ΔH_o^f (J/mole)
ZrF ₂	49	-962320
CrF ₂	57	-779479
MnF ₂	60	-803328
FeF ₂	61	-705841
CoF ₂	64	-671532
NiF ₂	67	-657725
PdF ₂	68	-468608

Table 4.2: Enthalpies of formation for known difluorides

It is evident from Table 4.2 that a linearly increasing trend exists for solid binary difluorides as the Mendeleev number increases. The data in Table 4.2 are represented graphically in Figure 4.2. A line is drawn through the points, showing good agreement

with the data. When the data for tri-, tetra- and penta- fluorides are plotted, similar results are seen (Figures 4.3, 4.4, and 4.5).

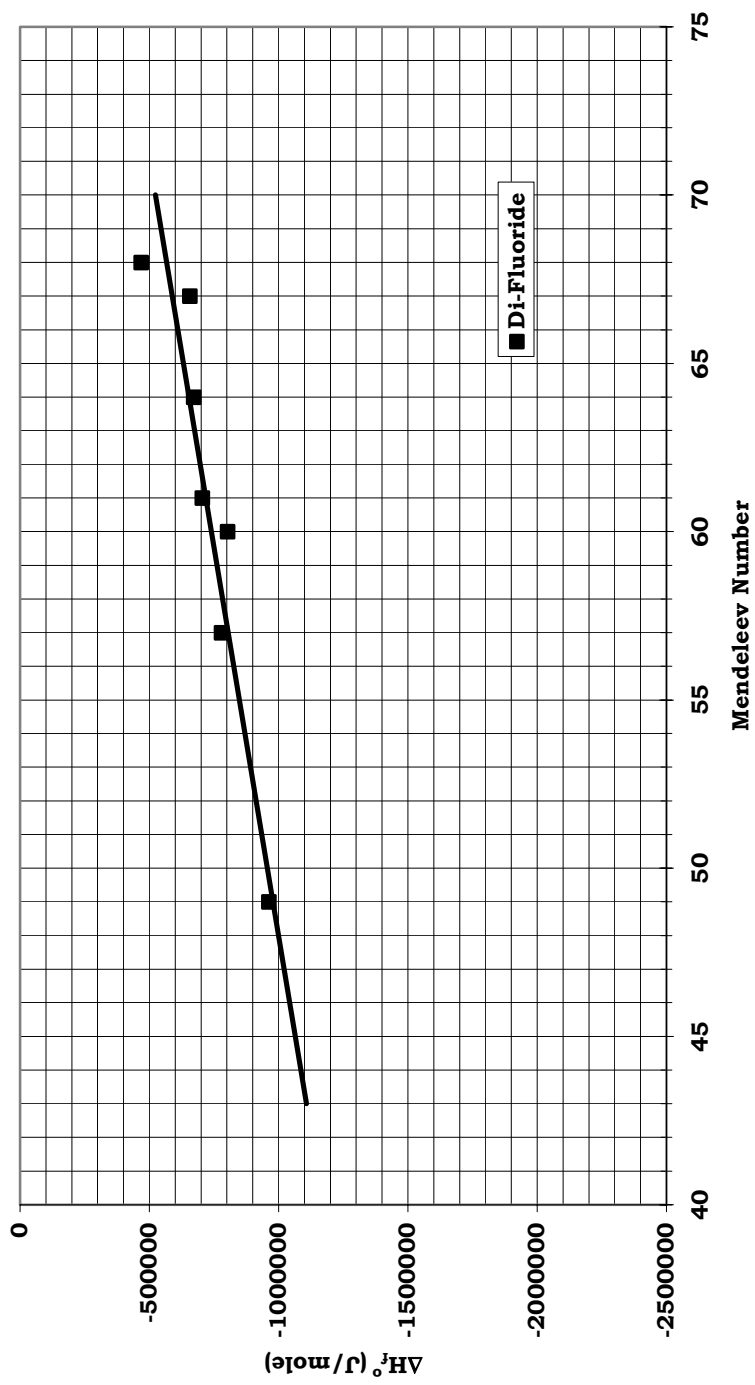


Figure 4.2: Enthalpy of formation vs. Mendeleev number for known difluorides

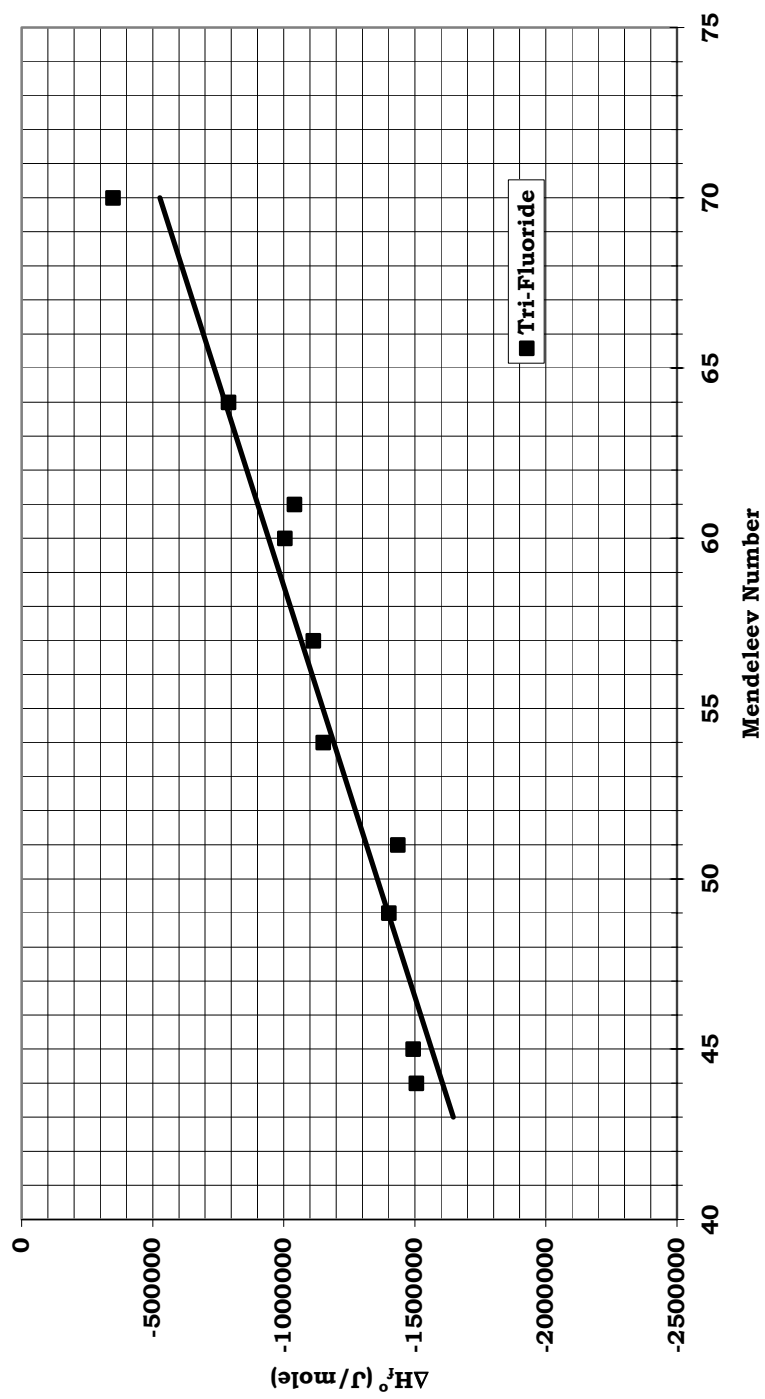


Figure 4.3: Enthalpy of formation vs. Mendeleev number for known trifluorides

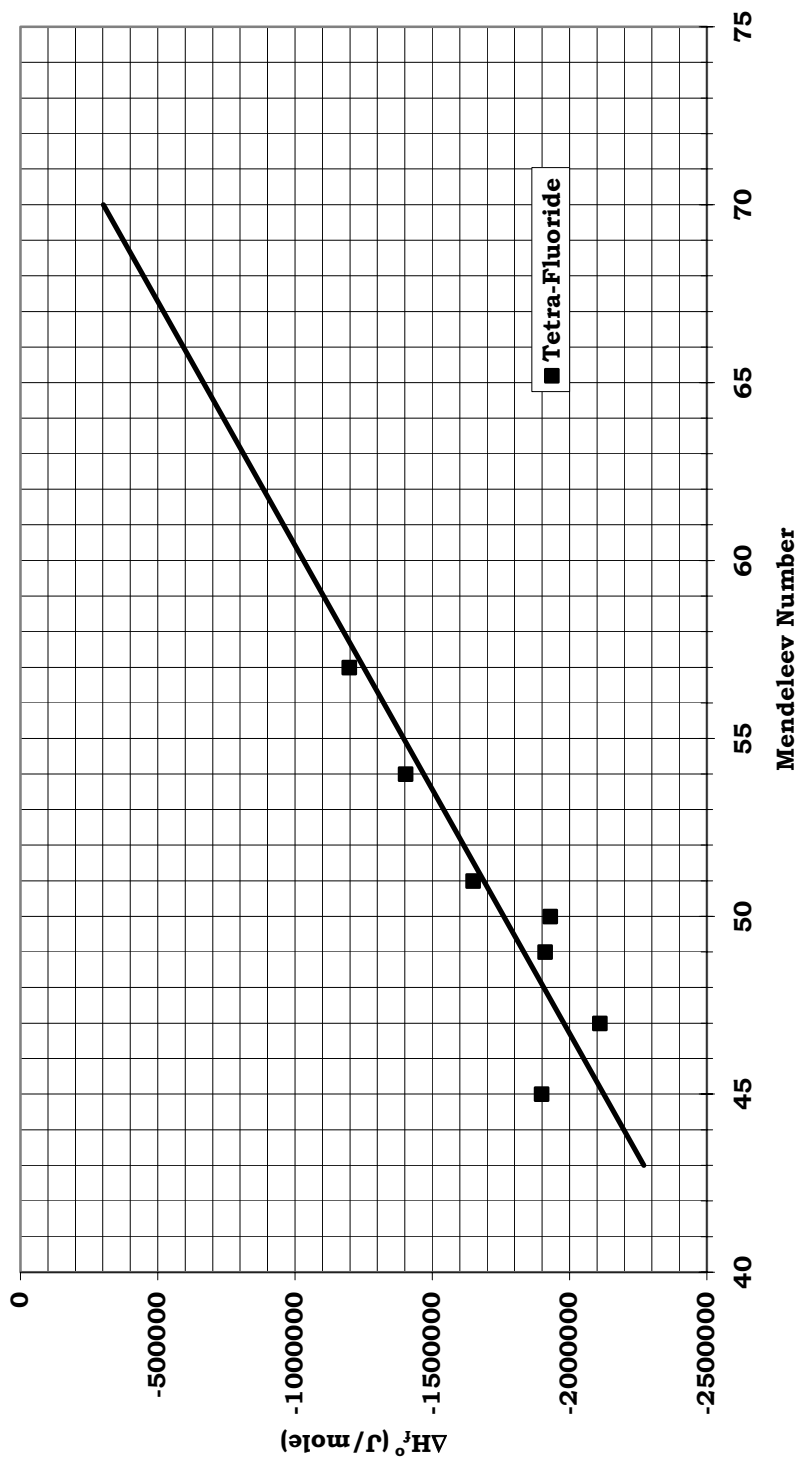


Figure 4.4: Enthalpy of formation vs. Mendeleev number for known tetrafluorides

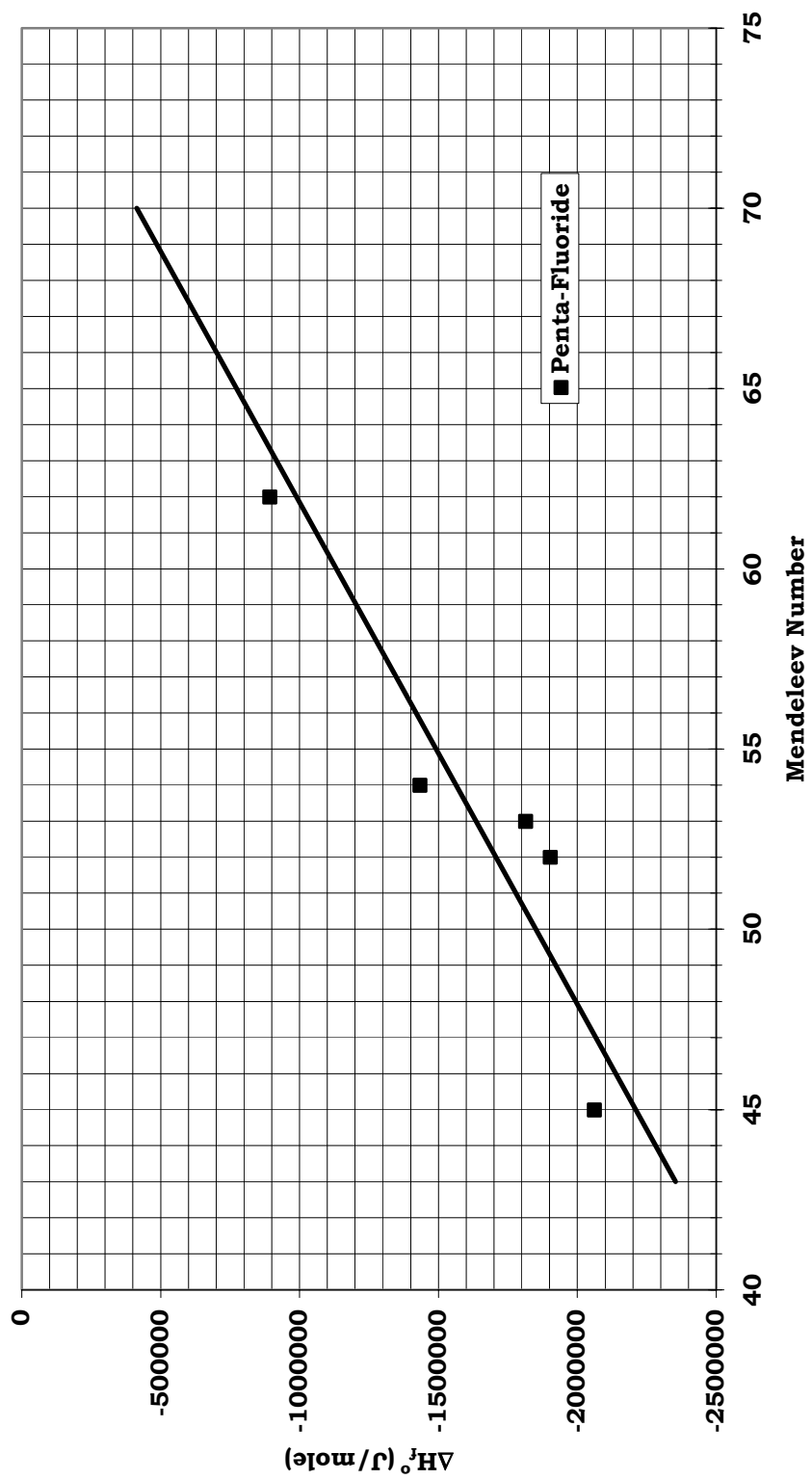


Figure 4.5: Enthalpy of formation vs. Mendeleev number for known pentafluorides

From Figure 4.1, Tc has a Mendeleev number of 59. A linear trend predicts a value for ΔH_o^f for TcF_5 is -1200 kJ/mol. This is in agreement with Glassner's value of -270 kcal/mol (-1130 kJ/mol). The value of -1200 kJ/mol is used for modeling.

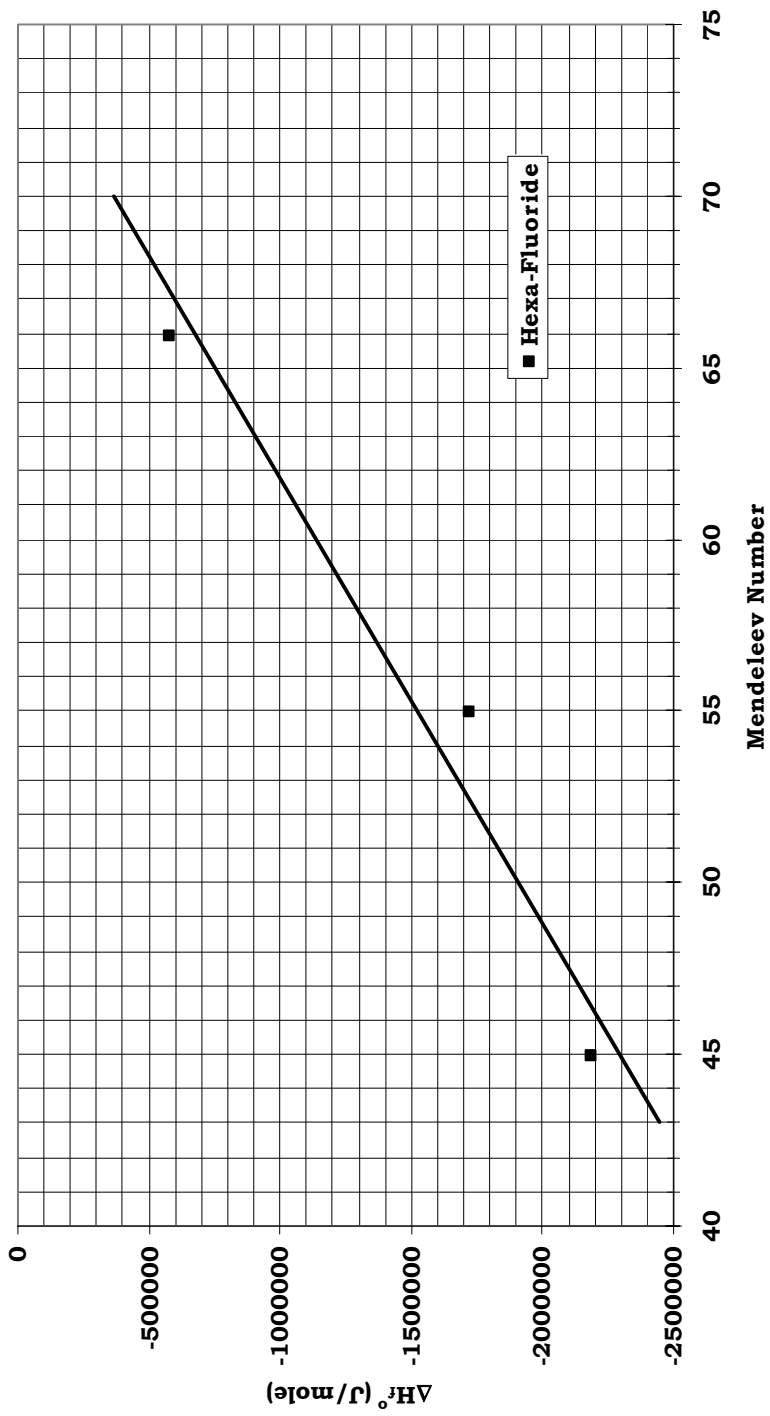


Figure 4.6: Enthalpy of formation vs. Mendeleev number for known hexafluorides

Data for hexafluorides are limited to UF_6 , WF_6 , and IrF_6 . Figure 4.6 shows a plot of these values. Assuming a linear trend predicts a value of -1210 kJ/mol for the enthalpy of formation of TcF_6 . This value is supported by Glassner's value of -300 kcal/mole (-1250 kJ/mol) for ΔH_o^f of TcF_6 (4). The value of -1210 kJ/mol will be used for calculations.

Other methods that could be explored to extrapolate data exist. Relationships between fluorides and chlorides, bromides, and even oxides and sulfides could be explored to determine the required thermochemical values. However, the data already provide the most direct chemical analogies.

CHAPTER 5

EQUILIBRIUM MODELING RESULTS

5.1 Input for modeling

User inputs for FACTSage® include the mass of each component, system pressure, system temperature, and the number of phases to consider. Models were run with excess F_2 and HF, at temperatures of 20 to 100 C and 20 to 500 C. The model was run to the higher temperature of 500 C to verify the formation and vaporization of the compounds that might be expected in the process. HF was modeled because it is used in the process of converting uranium oxide to uranium fluoride for uranium enrichment. That process requires a strong acid like HF to fluorinate the strong oxide UO_2 . HF reacts with the UO_2 to form UF_4 , which is then reacted with F_2 to form UF_6 . Since this model does not deal with oxides, it is expected that HF is not necessary (although the model results are presented anyway). Evidence exists that shows that Tc and F_2 will form TcF_6 in greater than 90% purity (12).

5.2 Explanation of results

The results from the model show only products with masses greater than $1\text{e-}5$ grams in the temperature range in question. The analysis assumes that the separation mechanism will involve manipulation of the vapor phase. For this reason, vapors are the only phase presented in the plots for clarity.

5.3 Results of HF reaction

Reaction of the metals in Table 3.1 with HF at temperatures from 20 to 100°C produces 12 vapors, most of which are varying compounds of hydrogen and fluorine (Figure 5.1). It is important to note that the HF reaction does not appear to form an appreciable amount of MoF_6 , SeF_6 , or TeF_6 . This is consistent with the UO_2 -HF reaction scheme mentioned earlier. Of course this reasoning means that HF should probably form a lower valence fluoride with Tc, such as TcF_5 , though the model predicts otherwise. This may indicate a need for more accurate thermochemical data for TcF_5 . As the temperature is increased to 500°C, many more vapors begin to appear (Figure 5.2), attesting to the reactivity of HF.

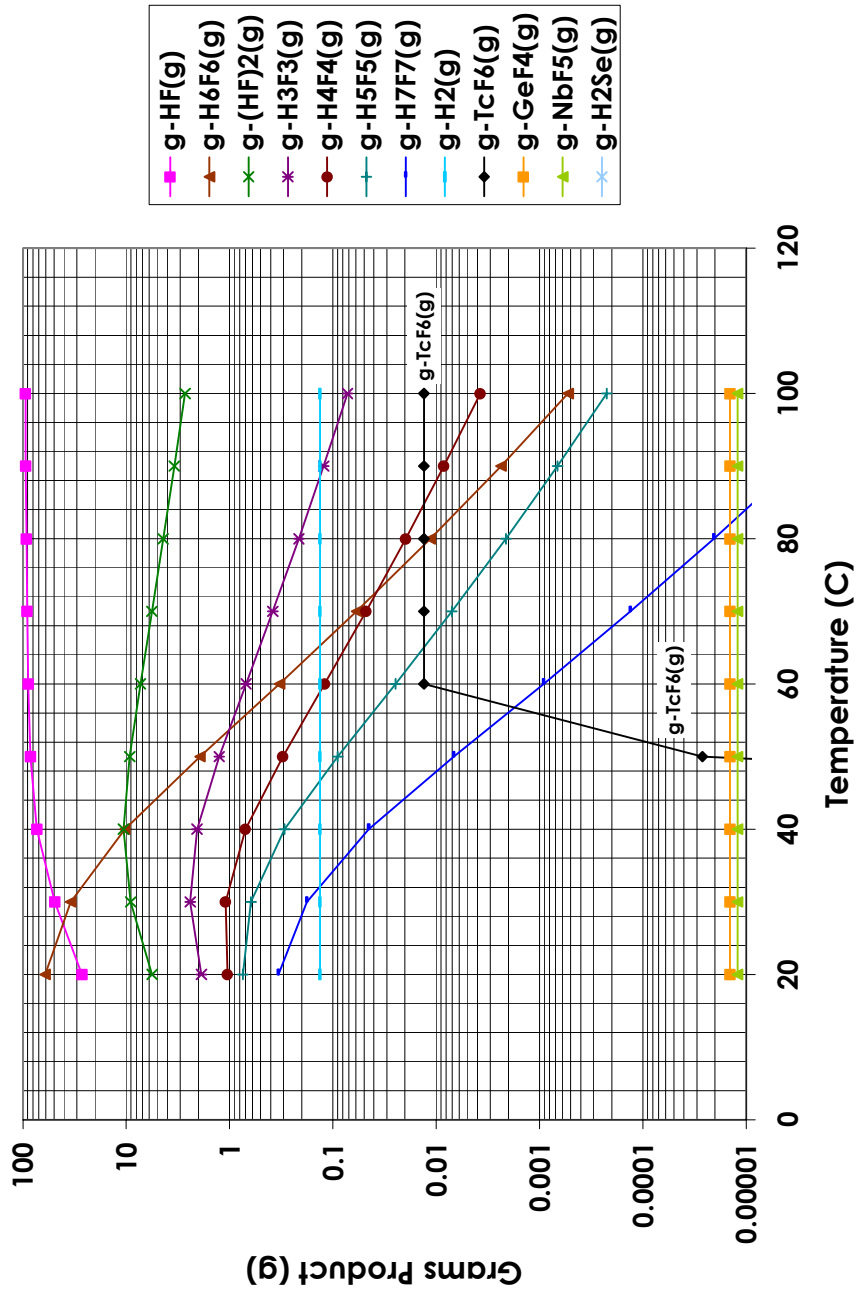


Figure 5.1: Major gaseous products from reaction of metals listed in Table 3.1

with excess HF, Temp = 20 – 100 C (F₂ gas omitted)

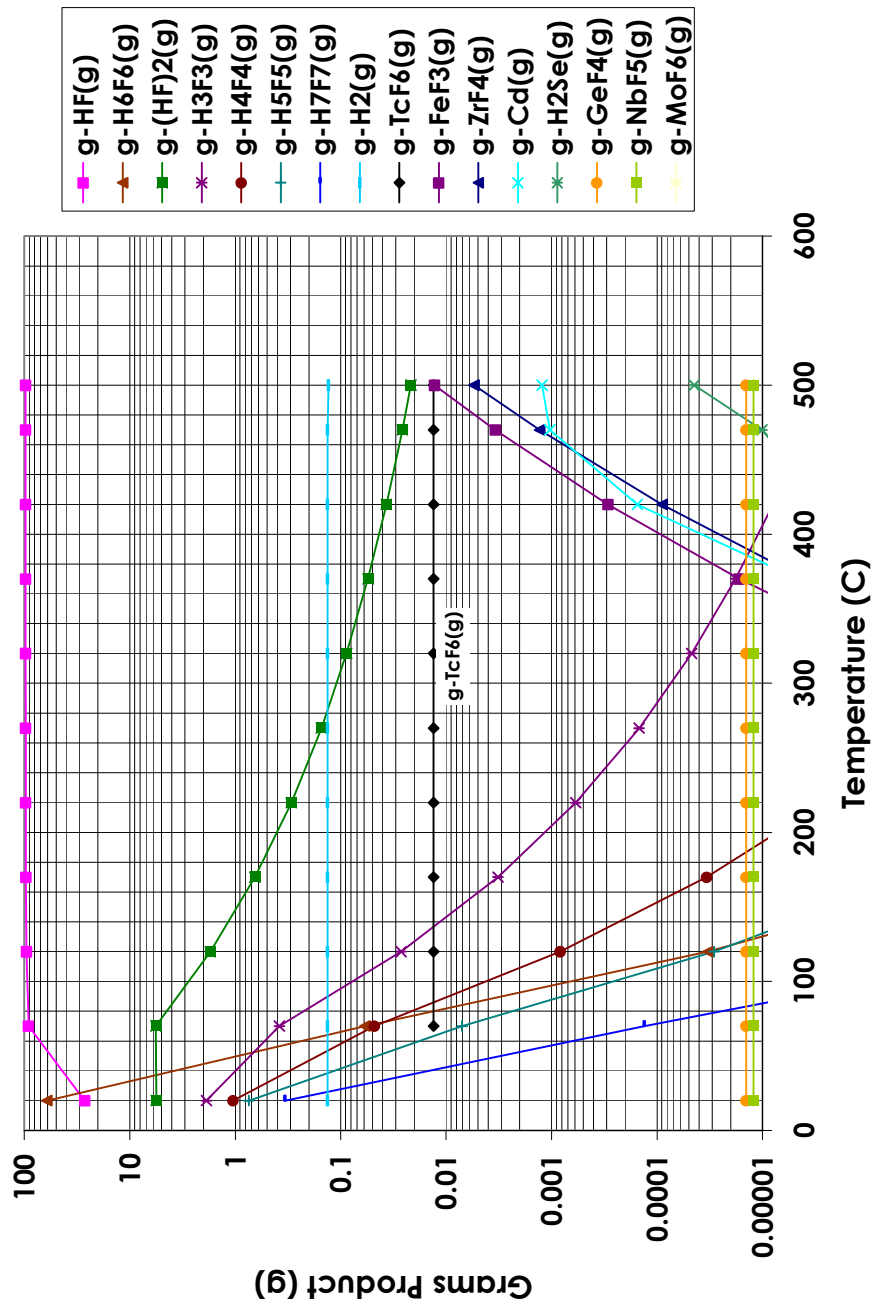


Figure 5.2: Major gaseous products from reaction of metals listed in Table 3.1 with excess HF, Temp = 20 – 500 C

5.4 Results of F₂ reaction

In the temperature range from 20 to 100C, excess F₂ and the elements from Table 3.1 react to form gaseous TcF₆, MoF₆, TeF₆, SeF₆ and minute amounts of GeF₄ and NbF₅ (Figure 5.3). For T = 20 to 500 C, more gaseous compounds are listed as products as the temperature approaches 500 C (Figure 5.4). This is an indication of the temperature limit that might be applied to the system, as more and more gaseous compounds lead to a more difficult separation. Note that Figures 5.3 and 5.4 do not display F₂ gas since its concentration does not appreciably vary with increasing temperature.

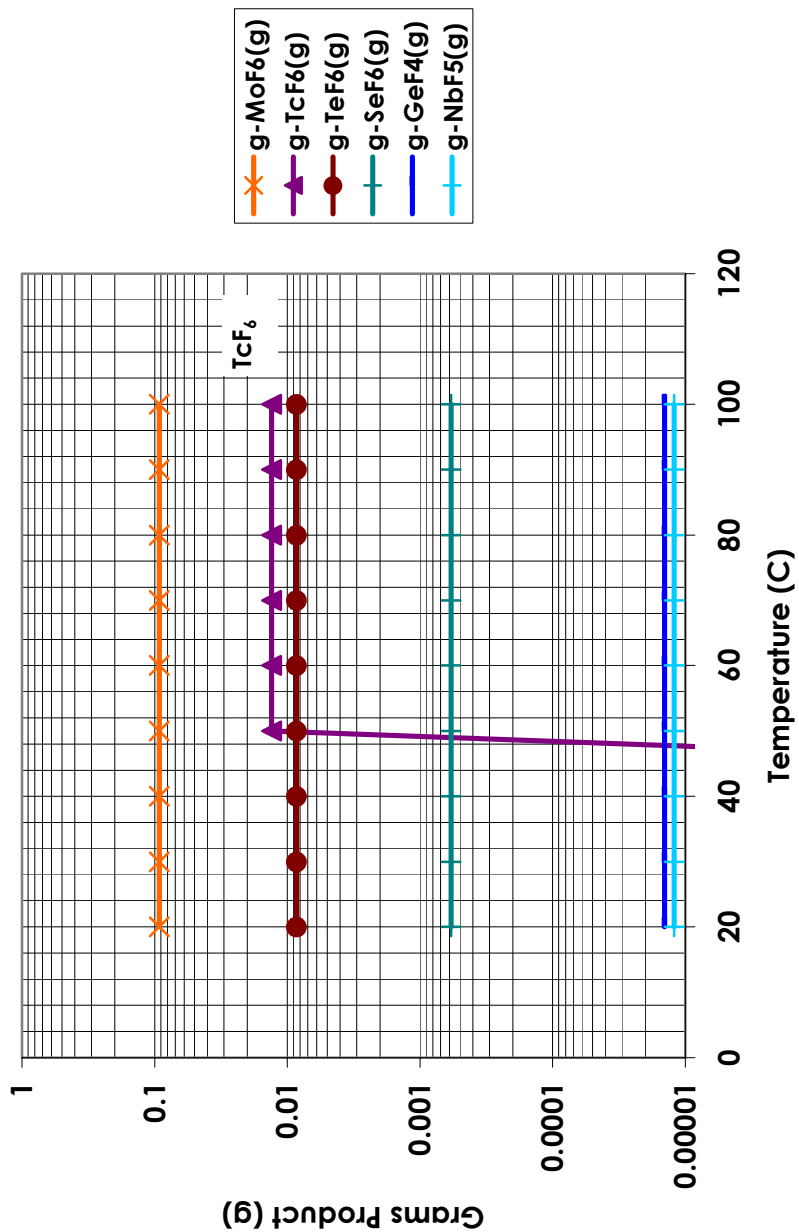


Figure 5.3: Major gaseous products from reaction of metals listed in Table 3.1

with excess F₂, Temp = 20 – 100 C (F₂ gas omitted)

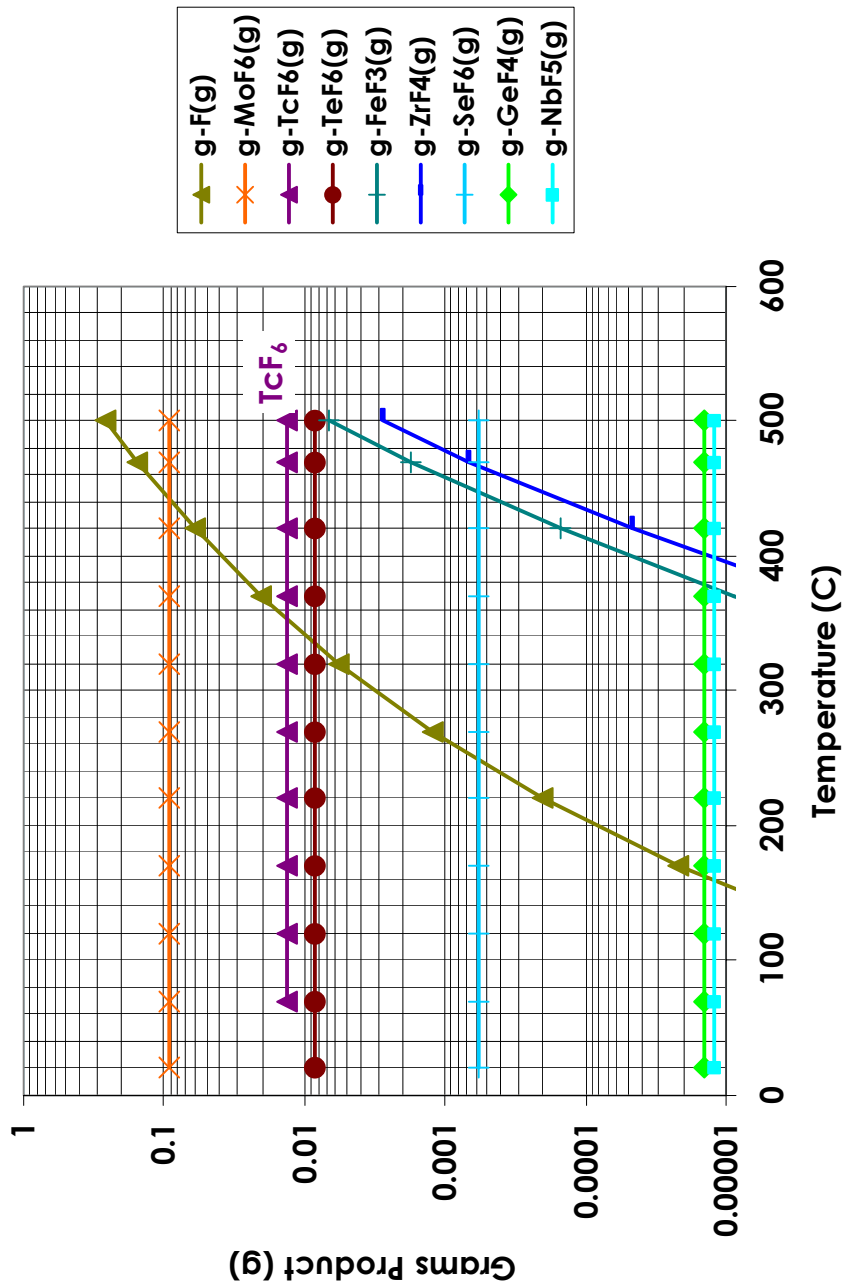


Figure 5.4: Major gaseous products from reaction of metals listed in Table 3.1

with excess F_2 , Temp = 20 – 500 C (F_2 gas omitted)

These trials support the idea that direct F₂ fluorination of the elements is enough to produce TcF₆ for a separation scheme and that this method can be used as a separation method. Indeed, Selig et al. reported direct fluorination of Tc metal was sufficient to produce TcF₆ with conversion rates of more than 90% (12). At a temperature range of 60–100 C, Tc can be removed from the majority of the AFCI fuel cladding elements and the majority of the fission products. However Mo, Te, Se and minute amounts of Ge and Nb are vaporized as fluorides as well, suggesting the need for additional separation processes.

Species	Mass Produced (g)
F ₂ (g)	9.735E+01
MoF ₆ (g)	9.223E-02
TcF ₆ (g)	1.316E-02
TeF ₆ (g)	8.514E-03
SeF ₆ (g)	5.840E-04
GeF ₄ (g)	1.433E-05
NbF ₅ (g)	1.213E-05

Table 5.1: Major gaseous products from the reaction of metals listed in Table 3.1 with Excess F₂, T = 60 – 100C

5.5 Isolation of TcF_6

The volatile TcF_6 must be separated from the other volatile fluorides, and then reduced to metallic Tc before it can be recycled to the transmutation scheme. Once the fluorination has proceeded to completion, a liquid nitrogen or dry ice cooled surface would condense the fluorides and allow the evacuation of the F_2 vapor. Once the fluorides are condensed, a simple fractional distillation scheme can be used to separate TcF_6 from the other fluorides. Table 5.2 lists the vapor pressures at 80 C of selected fluoride compounds predicted by FACTSage®. The very high volatilities of MoF_6 and TeF_6 compared to TcF_6 suggest that a separation is possible.

Compound	Vapor Pressure, mmHg at 80 C
TeF ₆	19650
MoF ₆	3303
TcF ₆	1628
NbF ₅	3.3

Table 5.2: Vapor pressures of selected compounds at 80 C

Pyrometallurgical processing has been suggested as a separation technique (8); however the low boiling points of hexafluorides make this option difficult to realize. As explained in chapter 2, the fluorides would electrotransport through a molten salt and collect on an electrode. The low boiling points of the hexafluorides make finding a suitable electrolyte difficult. Also, even if a suitable salt were found, MoF₆ and TcF₆ would be expected to behave very similarly, which would complicate the process further.

Another method of removing Tc is by the use of the MgF₂ trap. In UF₆ processing, the fluorinated UF₆ stream is passed through a column loaded with MgF₂ traps (5). This method is not suggested as it does not separate the Tc from Mo, however MgF₂ traps may be considered for some upstream processes.

Atomic vapor laser isotope separation is another technique that is used to separate chemically similar metallic species (18). This technique is probably too expensive to use for this application, but may warrant further investigation.

We conclude that distillation is the most promising of the techniques available for the separation of Tc from the other volatile fluorides.

5.6 Final Tc Waste Form

The technetium is to be metallic when it is returned to the transmutation scheme. Sadoway (3) gives an excellent review of methods of reducing halide metals. A brief overview will be presented here. Standard methods of reducing metallic halides to metals include electrolysis, metallothermic reduction, hydrogen reduction, and thermal decomposition. Electrolysis is probably not a viable option for the reasons cited in section 5.5.

Metallothermic reduction involves reacting the fluoride with a highly reactive metal such as magnesium, calcium, or sodium. In the Kroll process, $TiCl_4$ vapor is reacted with magnesium metal to produce solid Ti metal and molten MgCl. The recovered solid Ti is fairly impure and must be cleaned by vacuum distillation, which may unacceptably increase costs. In a similar process, solid UF_4 is reacted with calcium metal to produce U metal.

Reduction with hydrogen gas is used to produce tungsten metal from WCl_6 vapor. Control of the process variables allows production of tungsten particles of a specified size. Iron powder can also be produced from solid iron chloride via reaction with hydrogen. Tc metal is produced from the reaction of Tc_2S_7 with hydrogen (3).

Thermal decomposition of metal halides is an attractive route to the metal because it can be used to produce metals of very high purity. The process involves passing the low temperature metal halide vapor over a high temperature filament made of the desired metal. The halide vapor decomposes at the surface of the filament and the pure metal is deposited. Specifically, Tc metal is produced from the thermal decomposition of NH_4TcO_4 (3).

All three of the suggested methods for reducing TcF_6 to Tc metal warrant further investigation.

CHAPTER 6

CONCLUSIONS AND SUGGESTIONS FOR FURTHER WORK

6.1 Review

The objective of this thesis was to examine the possibility of using a fluoride volatility process to extract technetium from transmuted spent nuclear fuel. The thesis shows that fluoride volatility is certainly worthy of further investigation. The models show that F_2 is a proper fluorinating agent for this process, and will fluorinate Tc metal to volatile TcF_6 . There are other volatile fluorides produced along with TcF_6 which must be removed to obtain pure TcF_6 . This separation can be achieved through fractional distillation. The metal must then be reduced back to the metal for recycle into the transmuter. This can be accomplished with methods already used in industry. The main uncertainty with the feasibility of the concept is the kinetics involved in the fluorination step. The surrogate experiment is proposed to help answer some of the kinetics concerns. The success or failure of this experiment will indicate the probable performance of the fluorination of the AFCI fuel.

6.2 Suggestions For Further Work

Since most of the statements made here are results of computer models, and such models are only as good as their input, it would be very beneficial to have better thermochemical data for all noble metal fluorides. These data can be determined via experimentation and calculation.

A surrogate experiment could help determine if further study on fluoride volatility for this application is warranted. The data suggests that the real separation to be achieved is that of Tc from nearly all (96%) Zr, Fe and Cr. A mockup using Mo, which should behave in a similar manner to Tc, can be mixed with Zr, Fe and Cr to approximate the composition of the Pyro-B AFCI fuel. This fuel could be treated in the same manner as described above, and the results will indicate whether or not the proposed approach is worth further investigation. This idea is investigated extensively in appendix sections B and C.

The biggest impediment to the fluorination scheme actually working will be the kinetics of the reaction. During fluorination, a solid fluoride layer will form on the outer shell of the metal. This layer may prevent the fluorination of the inner layer of metal and subsequently not volatilize the Tc metal. To deal with this, the metal mix would ideally be ground/chopped fine to maximize the surface area to exposure to fluorine. Grinding the metal will undoubtedly prove difficult, however. It is also possible that the solid layer may flake off. It seems sensible, however, to develop a fluorination scheme that could remove the solid layer as it forms. The (turbulent?) upward flow of gas in a fluidized bed reactor could serve to remove the fluoride layer on the outer surface of the

metal. Another reactor is the molten salt reactor system. In this reactor, a fluoride salt will dissolve the solids as they form and ensure fluorination of all the metal.

Should the surrogate experiment results confirm the analyses performed in this thesis and indicate favorable kinetics, further work is necessary. A prototypic material should be developed for bench-scale testing. The composition should be as similar as possible to that of the AFCI fuel intended for the Pyro-B process (Table 3.1), including the use of Tc. This material can then be subjected to the fluorination scheme described in this thesis to verify that Tc can be separated. If these tests indicate that Tc can be separated in AFCI fuel by fluorination, then full scale engineering development is necessary.

A complete conceptual design would guide the full development of the process. This would include a preliminary cost analysis and a fully developed flowsheet for the process. These suggestions could all be performed with the equipment and materials currently at ANL, and could make excellent theses for future students.

BIBLIOGRAPHY

1. *A Roadmap for Developing Accelerator Transmutation of Waste Technology*. A report to Congress. DOE/RW-0519. October, 1999.
2. Data from HSC Database, provided by Argonne National Laboratory.
3. Encyclopedia of Materials Science and Engineering. Ed. Michael B. Bever. Pergamon Press, Cambridge, MA. 1986.
4. Glassner, Alvin. *The Thermochemical Properties of the Oxides, Fluorides and Chlorides to 2,500°K*. ANL-5750, U.S. Atomic Energy Commission, 1957.
5. Gollither, W.R. *Process for Separation and Recovery of Volatile Fluoride Impurities from Uranium Hexafluoride Containing the Same*. US Patent #3,165,376. Jan. 12, 1965.
6. Gordon, S. and McBride, B. J. *Computer Program for Calculation of Complex Chemical Equilibrium Compositions and Applications. I. Analysis*. Oct. 1994, NASA RP 1311.
7. Information on the FACTSage® program is currently available at: www.factsage.com
8. J.J. Laidler, et. al. *Chemical Partitioning Technologies for an AFCI System*. Progress in Nuclear Energy. Vol. 38 (1-2), 65-79, 2001.
9. Lee, Hae-Geon. *Chemical Thermodynamics for Metals and Materials*. Imperial College Press, London. 1999.
10. *Nuclear Fuel Cycle Technologies for a Long-Term Stable Supply of Nuclear Energy*. Hitachi Review. Vol. 50 (3), 89-94, 2001.
11. Osbourne, Darrell W., et. al. *Heat capacity, entropy, and Gibbs energy of technetium hexafluoride between 2.23 and 350 K; magnetic anomaly at 3.12 K; mean β energy of ^{99}Tc* . Journal of Chemical Physics. 69(3), 1 Feb. 1978. 1108 – 1118.

12. Selig, H., Chernick, C. L., Malm, J. G., *The preparation and properties of TcF₆*. Journal of Inorganic Nuclear Chemistry. 19 (1961) 377.
13. Spencer, P.J. Estimation of thermodynamic data for metallurgical applications. Thermochemica Acta. 314 (1998) 1-21.
14. Knief, Ronald A. Nuclear Engineering: theory and technology of commercial nuclear power. Hemisphere Pub. Corp. New York. 1992.
15. Pasamehmetoglu, Kemal O. *AAA Program: Overview of the Transmutation Science Activities*. LA-UR-02-1002. Los Alamos National Laboratory. March, 2002.
16. Laidler, J.J. et al. *Development of Pyroprocessing Technology*. Progress in Nuclear Energy. Vol. 31 (1-2), 131-140, 1997.
17. *CRC Handbook of Chemistry and Physics*. CRC Press. Cleveland, OH. 2002.
18. Atomic Vapor Laser Isotope Separation overview:
<http://www.llnl.gov/str/Hargrove.html>.

APPENDIX A

THEORY FOR PREDICTING CHEMICAL EQUILIBRIUM

A system is in equilibrium when the internal energy of the system is minimized and its entropy is maximized. The enthalpy of a system is defined as the internal energy of a system plus the product of its pressure and volume:

$$H = U + PV \quad (\text{A.1})$$

where H is the enthalpy of the system, U is internal energy, P is pressure and V is volume. Differentiating this term at constant pressure yields:

$$dH = dU + PdV \quad (\text{A.2})$$

With the first two laws of thermodynamics:

$$dU = dq_{rev} - dw_{rev} \quad (\text{A.3})$$

$$dS = \frac{dq_r}{T} \quad (\text{A.4})$$

where S is the entropy of the system. Equation A.2 can be written as:

$$dH - TdS = PdV - dw_{rev} \quad (\text{A.5})$$

It is important to remember that equation A.4 is valid only if the system is at equilibrium, otherwise the dS term will continually increase. The left hand side of equation A.5 is defined as dG , the Gibbs energy differential, from

$$G = H + TS \quad (\text{A.6})$$

$$dG = dH - TdS \quad (\text{A.7})$$

Therefore, dG is written as

$$dG = PdV - dw_{rev} \quad (\text{A.8})$$

and since dw_{rev} is defined as

$$dw_{rev} = PdV - dw_{add} \quad (\text{A.9})$$

where dw_{add} is considered additional work, but we've restricted this system to PV work, so dw_{add} is zero. This leaves:

$$dG = 0 \quad (\text{A.10})$$

So it is shown that the Gibbs energy of a system at equilibrium (maximized entropy and minimized energy) will have reached a minimum and dG must be zero. Again, dG

describes the tendency of a system to maximize its energy (dH) and minimize its entropy (dS).

G for a compound (G_i) is a function of temperature, pressure and composition. However at constant T and P, G becomes a function only of composition:

$$G = G(n_i) \quad (\text{A.11})$$

or

$$dG_i = \left(\frac{\delta G}{\delta n_i} \right) dn_i \quad (\text{A.12})$$

Equation A.12 represents the differential of the Gibbs energy of a species with respect to its concentration within a mixture. The sum of these differentials is the Gibbs energy of the entire mixture:

$$dG_{mix} = \sum_{i=1}^n \left(\frac{\delta G}{\delta n_i} \right) dn_i \quad (\text{A.13})$$

At equilibrium, Eq. A.13 is equal to zero as above. $\delta G/\delta N_i$ is the chemical potential of component i of the system. Equation A.13 shows that the sum of all the dG terms in a system must be zero at equilibrium, which is somewhat intuitive. The G term for an individual species is written similarly to equation A.6:

$$G_i = H_i - TS_i \quad (\text{A.14})$$

The H term can be expanded such that it is in terms of enthalpy of formation, and the entropy can be written with the pressure correction for ideal gases. With these rearrangements, equation A.13 can be written as

$$dG_{mix} = \sum_{i=1}^n \left[G_i^* + RT \left(\ln \left(\frac{N_i}{N} \right) + \ln \left(\frac{P_i}{P_0} \right) \right) \right] dn_i \quad (\text{A.15})$$

where R is the gas constant, P_i is the partial pressure of component i, N_i is the number of moles of component i, N is the total number of moles of component i, and G_i^* is defined as the Gibbs free energy of formation at temperature T

$$G_i^* = H_{f,i}^0 + (H_i - H_{0,i}) - TS_i^0 \quad (\text{A.16})$$

In this equation,

$H_{f,i}^0$ = standard formation enthalpy

H_i = enthalpy at temperature T

$H_{0,i}$ = enthalpy at 298K

S_i^0 = entropy at temperature T

**However for this model, G_i^* will be either predicted or taken from tabulated values.*

Equation A.15 describes the entire chemical system in full, and assuming T and P are specified, the only unknowns are the N_i 's, which are manipulated to find a solution to the equation, which specifies equilibrium composition of the system.

Constraints must be applied to equation A.15 to determine the appropriate N_i 's. One constraint is that the total number of moles of each element in the system must remain constant. This can be stated mathematically as:

$$\sum_{i=1}^{NS} a_{i,j} N_i - b_j \quad (\text{A.17})$$

where $a_{i,j}$ is the number of atoms of element j per molecule i and b_j is the total moles of element j in the system (defined initially). There will be one of these equations for every element in the system.

A solution to equation A.15 with the constraint of equation A.17 can be determined using Lagrange multipliers. A review of Lagrange multipliers is provided now:

Lagrange Theorem: If $f(x,y)$ is constrained with $g(x,y)=0$, there is a number λ that will satisfy the equation

$$L(x,y,\lambda) = f(x,y) + \lambda g(x,y)$$

λ is found by solving the equations

$$\frac{\delta L}{\delta x} = \frac{\delta f}{\delta x} + \lambda \frac{\delta g}{\delta x} = 0 \quad (\text{A.18})$$

$$\frac{\delta L}{\delta y} = \frac{\delta f}{\delta y} + \lambda \frac{\delta g}{\delta y} = 0 \quad (\text{A.19})$$

$$\frac{\delta L}{\delta \lambda} = g(x, y) = 0 \quad (\text{A.20})$$

For these equations:

$$dG_{mix} = \sum_{i=1}^{N_s} \left[G_i^* + RT \left(\ln \left(\frac{N_i}{N} \right) + \ln \left(\frac{P_i}{P_0} \right) \right) \right] dn_i \quad (\text{A.21})$$

$$\sum_{i=1}^{N_s} a_{i,j} N_i - b_j \quad (\text{A.22})$$

the Lagrangian equations are

$$L = \frac{\delta G_i}{\delta n_i} + \lambda_j \sum_{i=1}^{N_s} a_{i,j} N_i - b_j \quad (\text{A.23})$$

$$\frac{\delta L}{\delta n_i} = \frac{\delta G_i}{\delta n_i} + \sum_{j=1}^{N_e} a_{i,j} \lambda_j \quad (\text{A.24})$$

$$\frac{\delta L}{\delta \lambda_i} = b_j - \sum_{i=1}^{N_s} a_{i,j} N_i = 0 \quad (\text{A.25})$$

where N_e is the number of elements and N_s is the number of species (including elements) in the system. There will be an equation A.24 for every species and an equation A.25 for every element in the system.

The equations above are simplified by noting that

$$\frac{\delta G_i}{\delta n_i} = \mu_i \quad (\text{A.26})$$

where μ_i is the chemical potential of compound i , but at a standard state,

$$\mu_i^0 \equiv \Delta G_{f,i}^0 \quad (\text{A.27})$$

so here $\frac{\delta G_i}{\delta n_i}$ will be replaced with $\Delta G_{f,i}$. The lack of a 0 superscript on the ΔG term

simply implies that compound i is not at standard state, implying that a correction factor must be applied to the $\Delta G_{f,i}^0$ term.

Solving the resulting equations:

$$\frac{\delta L}{\delta n_i} = \Delta G_{f,i} + \sum_{j=1}^{N_e} a_{i,j} \lambda_j = 0 \quad (\text{A.28})$$

and

$$\frac{\delta L}{\delta \lambda_i} = b_j - \sum_{i=1}^{N_s} a_{i,j} N_i = 0 \quad (\text{A.29})$$

determine equilibrium composition.

A final constraint is that the total number of moles in the system must equal the sum of the individual mole numbers:

$$\sum_{i=1}^{N_s} N_i - N_{tot} = 0 \quad (\text{A.30})$$

where N_{tot} is the total number of moles of the system. The unknowns in equations A.25, A.28 and A.30 are the N_i 's, λ_i 's, and N_i , however there are exactly this many equations, so the system is defined.

To solve this defined system, the equations are first written in matrix form. To do this, the $\Delta G_{f,i}$ term is expanded to account for non-ideal conditions:

$$\Delta G_{f,i} = \Delta G_{f,i}^0 + RT \ln \frac{N_i}{N} + RT \ln \frac{P}{P_0} \quad (\text{A.31})$$

Dividing by RT, equation A.28 becomes:

$$\frac{\Delta G_{f,i}^0}{RT} + \ln \frac{N_i}{N} + \ln \frac{P}{P_0} + \sum_{j=1}^{N_e} a_{i,j} \frac{\lambda_j}{RT} = 0 \quad (\text{A.32})$$

Starting with an initial guesses for N_i and λ_j , the ΔN_i and $\Delta \lambda_j$ terms are calculated by solving equation A.33:

$$\sum_{i=1}^{N_s} \frac{\delta(f(x_i))}{\delta x_i} \Delta x_i = [F(X)] \quad (\text{A.33})$$

for Δx_i , where the $f(x_i)$ equations are equations A.29, A.30 and A.32 with variables $\Delta \ln N_i$, $\Delta \ln N$ and $\Delta \lambda_j/RT$, respectively. $[F(X)]$ is a matrix formed by the sum of the left side of the equation. Applying equation A.33 to equations A.29, A.30 and A.32 gives:

$$\sum_{i=1}^{N_s} a_{i,j} N_i \ln \Delta N_i = \sum_{i=1}^{N_s} a_{i,j} N_i - b_j \quad (\text{A.34})$$

$$\sum_{i=1}^{N_s} N_i \ln \Delta N_i - N \ln \Delta N = N - \sum_{i=1}^{N_s} N_i \quad (\text{A.35})$$

$$\Delta \ln N_i - \Delta \ln N - \sum_{i=1}^{N_e} a_{i,j} \frac{\Delta \lambda_i}{RT} = -\frac{\Delta G_f^0}{RT} - \ln \left(\frac{N_i}{N} \right) - \ln \left(\frac{P}{P_0} \right) + \sum_{i=1}^{N_e} a_{i,j} \frac{\lambda_i}{RT} \quad (\text{A.36})$$

So the algorithm for calculating chemical equilibrium is to guess initial values for N_i and λ_i , calculate the ΔN_i and $\Delta \lambda_i$ terms, add those to the N_i and λ_i terms and repeat the process until the Δ terms approach zero (convergence is reached).

The method described here is adapted from the approaches taken by Gordon et al. (6) and Lee (9).

APPENDIX B

SUGGESTED SURROGATE EXPERIMENT

B.1 Background

Testing for a fluorination scheme of the size suggested by this thesis would be complicated and expensive. Assembling an exact replica of the metallic mix listed in Table 3.1 would be very expensive. The radiation field and toxicity of the metals also presents a safety concern. For these reasons, a surrogate experiment that closely approximates the behavior of the mix would be beneficial. A close examination of the elements in Table 3.1 shows that Zr, Fe and Cr comprise 96% of the mass. The gaseous compounds after F_2 reaction are mostly Mo. This is shown graphically in Figure B.1

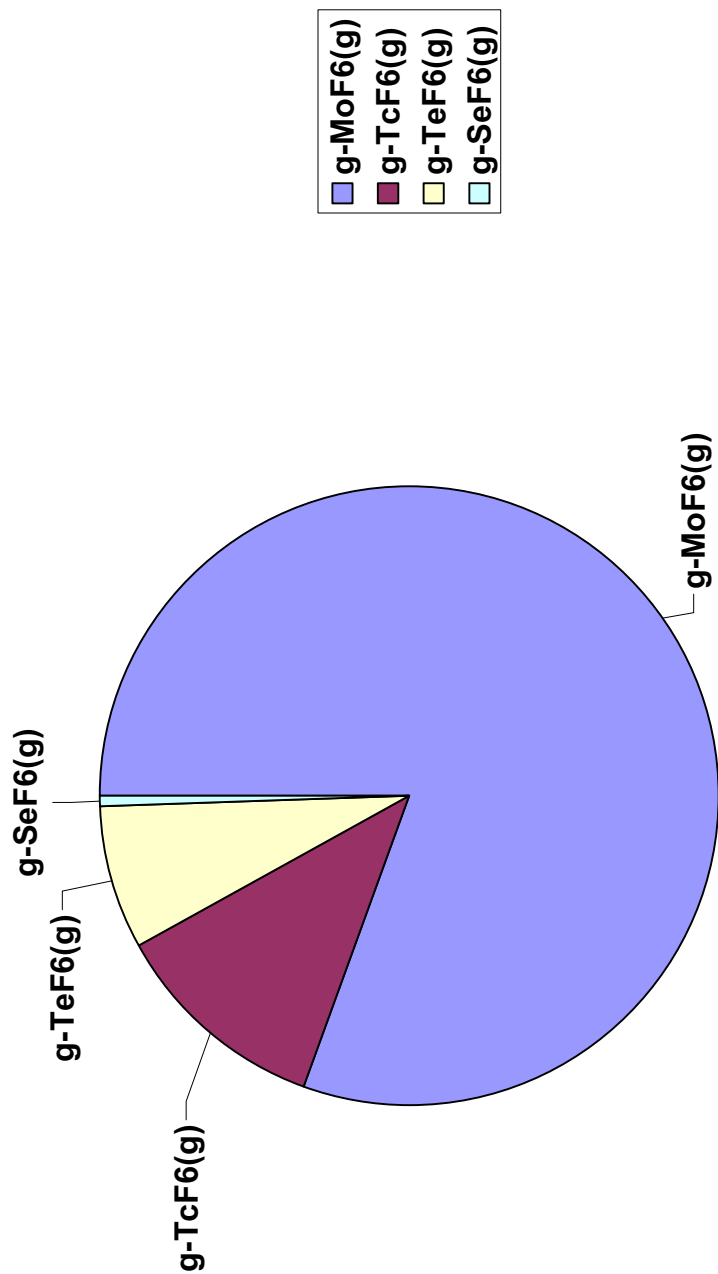


Figure B.1: Major gaseous products from F₂ reaction with metals in Table 3.1

The separation to be achieved is essentially Mo, Tc and Te from the much greater mass of Zr, Fe, and Cr. Because Mo, Tc and Te have quite similar chemistry, a non-radioactive surrogate experiment could be performed for the proof of principal experiment using Mo to simulate Tc behavior. The experiment could be performed using the four principal constituents Mo, Zr, Fe and Cr.

B.2 Experimental Setup

Argonne National Laboratory (ANL) has a static fluorine chamber which is being considered for use in this experiment. The setup is a metal (Monel) cylinder in a fume hood. The cylinder is loaded with feed, evacuated, and flooded with up to 1000 torr of F₂ gas. This atmosphere can be maintained at a temperature of up to 100 C. The feed is allowed to react with the F₂ gas for a predetermined amount of time. Once equilibrium is reached, vapor samples can be taken and stored in specially designed vials that are inert to fluorine. Cooling of the vials to liquid nitrogen temperatures will condense the fluorides. F₂ can then be evacuated. The solid fluorides can then be analyzed with a mass spectrometer.

A packed bed setup might also be used. The solid metal is placed on a screen in a tube and a specific quantity of F₂ is passed through the tube. The volatile products could

then be collected on a cold trap downstream. The flowing F_2 gas ensures the volatile products would transport.

The ANL setup is to be considered in this thesis because of its convenience and the fact that it is already constructed.

B.3 Experimental Uncertainties

This surrogate experiment has obvious advantages of cost, time and safety. There are some uncertainties that must be addressed in an experiment of this type. First of all, the validity of a surrogate is always questionable. There may be complexes formed between the metals themselves and/or the fluorine that have not yet been documented. Whether these complexes would retard the formation of TcF_6 is unclear.

Once the MoF_6 has been collected, it would be convenient to store it in glass for visual inspection. However, MSDS sheets indicate that MoF_6 should only be stored in metal containers.

The composition of the feed should be approximated as closely as possible to the AFCI mix (Table 3.1). A composite of alloys will be suggested later in this chapter.

The temperature should be close to that suggested in chapter 5 (60 – 100 C). A 212 F temperature limit is imposed by the equipment.

F₂ is to be in large excess. The partial pressure of F₂ is limited by the volume of the equipment. The ANL fluorination chamber has a volume of 4.1 L. This value can be used to determine the maximum amount of F₂ gas that can be used.

Another uncertainty is oxygen contamination. If the metal were to interact with O₂, it may form a protective oxide layer on the metal surface. This oxide layer would make fluorination difficult. In the full-scale Pyro-B process, great care will be taken to avoid any contact with oxygen. The same care should be taken in this experiment. Regardless, the possibility of O₂ contamination is considered in the following sections of this chapter.

It is important to note that the time it takes to reach equilibrium is not determined by FACTSage®, so the proper time of reaction will have to be determined experimentally.

Full fluorination of all the metal feed may be prevented should a layer of solid fluoride form on the feed surface. To avoid this, the feed particle size should be reduced as much as possible to maximize surface area.

It should be noted also that this experiment addresses only the separation of the volatile fluorides from the non-volatile solids. This experiment would not address the isolation of Tc.

Finally, any solid fluorides will have associated vapor pressures which may indicate their potential to contaminate the vapor. The vapor pressures of the solid fluorides should be researched and noted if they prove to be too high.

APPENDIX C

MODELING OF THE SURROGATE EXPERIMENT

C.1 Feed composition

The composition of the feed is approximated by a mix of stainless steel #316 (SS-316) and Zircaloy-2. 50.3% SS-316 and 49.7% Zircaloy-2 sufficiently approximates the processed AFCI fuel. There is no Tc in the SS-316/Zircaloy mix, and the disproportionate amount of Ni should be noted. The exact compositions are shown graphically in Figures C.1 and C.2 and listed in Table C.1. A 10 gram sample is assumed for compatibility with the size of the ANL equipment.

Compositions of SS-316/Zircaloy-2 Mixture vs. Spent Processed ATW Fuel

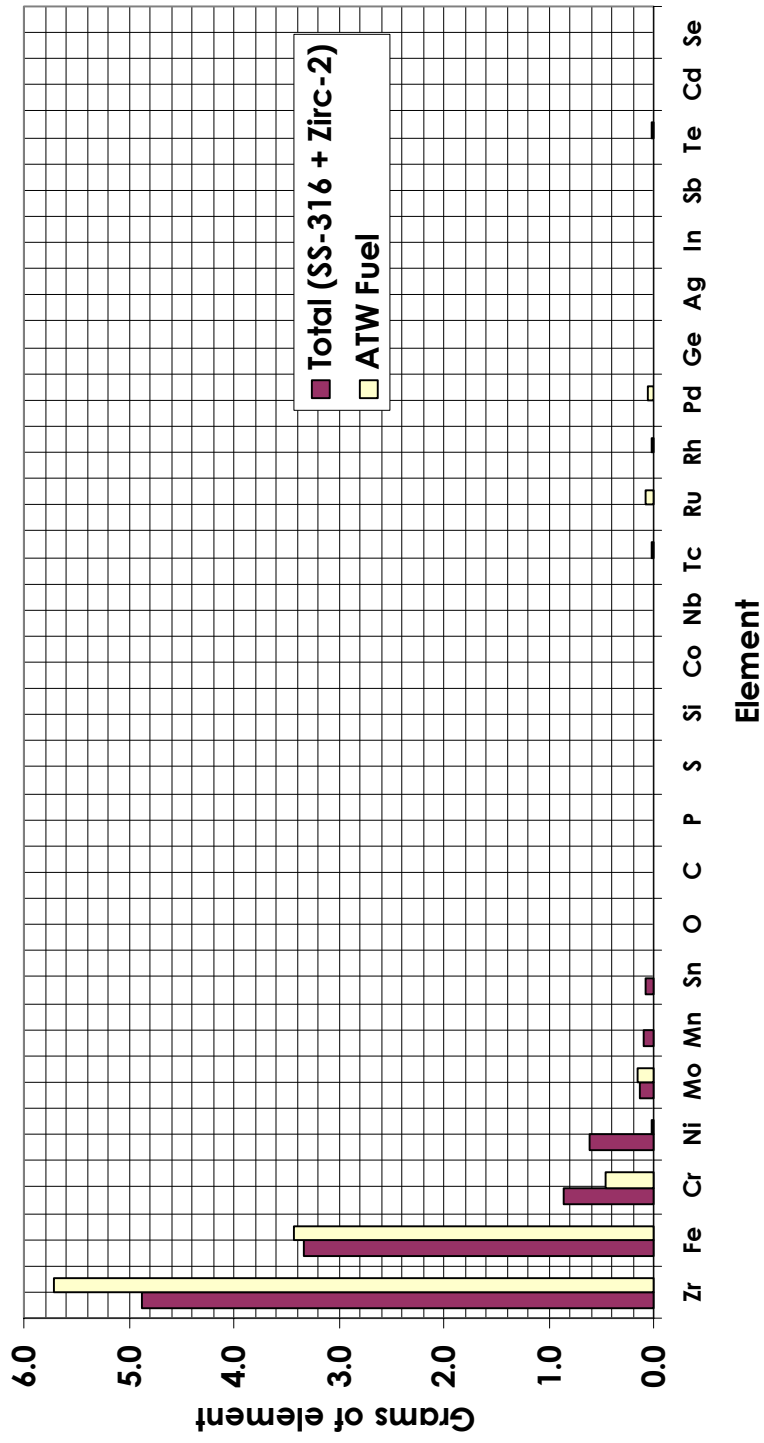


Figure C.1: Compositions of SS-316/Zircaloy-2 mixture vs. theoretical feed for fluorination scheme

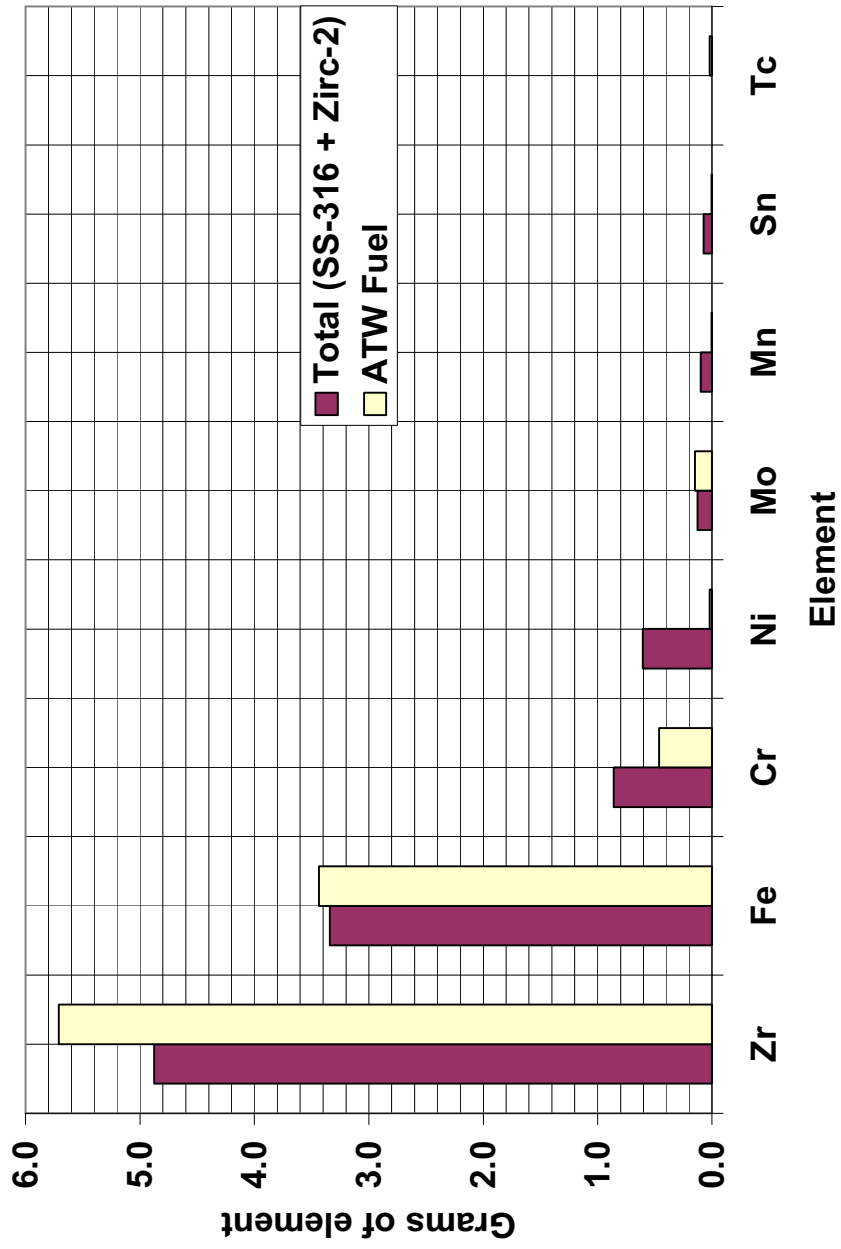


Figure C.2: Major elements of SS-316/Zircaloy-2 mixture vs. theoretical feed for fluorination scheme

Element	SS-316 + Zirc-2 (grams)	AFCI Fuel (grams)	Difference (grams)
Zr	4.876	5.709	0.832
Fe	3.341	3.437	0.096
Cr	0.860	0.464	0.396
Ni	0.606	0.020	0.586
Mo	0.126	0.148	0.022
Mn	0.101	0.004	0.097
Sn	0.075	0.003	0.071
O	0.006	0.000	0.006
C	0.004	0.000	0.004
P	0.002	0.000	0.002
S	0.002	0.000	0.002
Si	0.002	0.000	0.002
Co	0.000	0.000	0.000
Nb	0.000	0.000	0.000
Tc	0.000	0.021	0.021
Ru	0.000	0.079	0.079
Rh	0.000	0.027	0.027
Pd	0.000	0.059	0.059
Ge	0.000	0.000	0.000
Ag	0.000	0.006	0.006

In	0.000	0.000	0.000
Sb	0.000	0.001	0.001
Te	0.000	0.016	0.016
Cd	0.000	0.004	0.004
Se	0.000	0.001	0.001
<u>TOTAL</u>	<u>10.000</u>	<u>10.000</u>	

Table C.1: Compositions of SS-316/Zircaloy-2 mixture vs. theoretical feed for fluorination scheme

C.2 FACTSage® Modeling Input and Results

The SS-316/Zircaloy-2 metal feed defined in Table C.1 was input into FACTSage® with a constrained volume of 4.8 L. The proper amount of F₂ needed to achieve a pressure of about 1 atm was determined first. HF was not investigated as a potential fluorinating agent. The equipment in this experiment will not tolerate pressures higher than 1000 torr, so it seems reasonable to aim for a pressure of 1 atm. Running trials with varying amounts of F₂ predicts that 14.6 grams F₂ input will reach about 1atm in a 4.1L container. F₂ is in excess if the initial amount of F₂ is greater than about 10g, so its partial pressure should be roughly equal to the total system pressure. Figure C.3 shows the varying masses of solids and vapors as the amount of initial fluorine is increased. Note that after 10g initial F₂ the mass of solid does not change and the amount of vapor increases in direct proportion to the amount of F₂ vapor input. This indicates F₂ is in excess. Table C.2 lists the system pressure and the masses of the major gaseous products from the reaction.

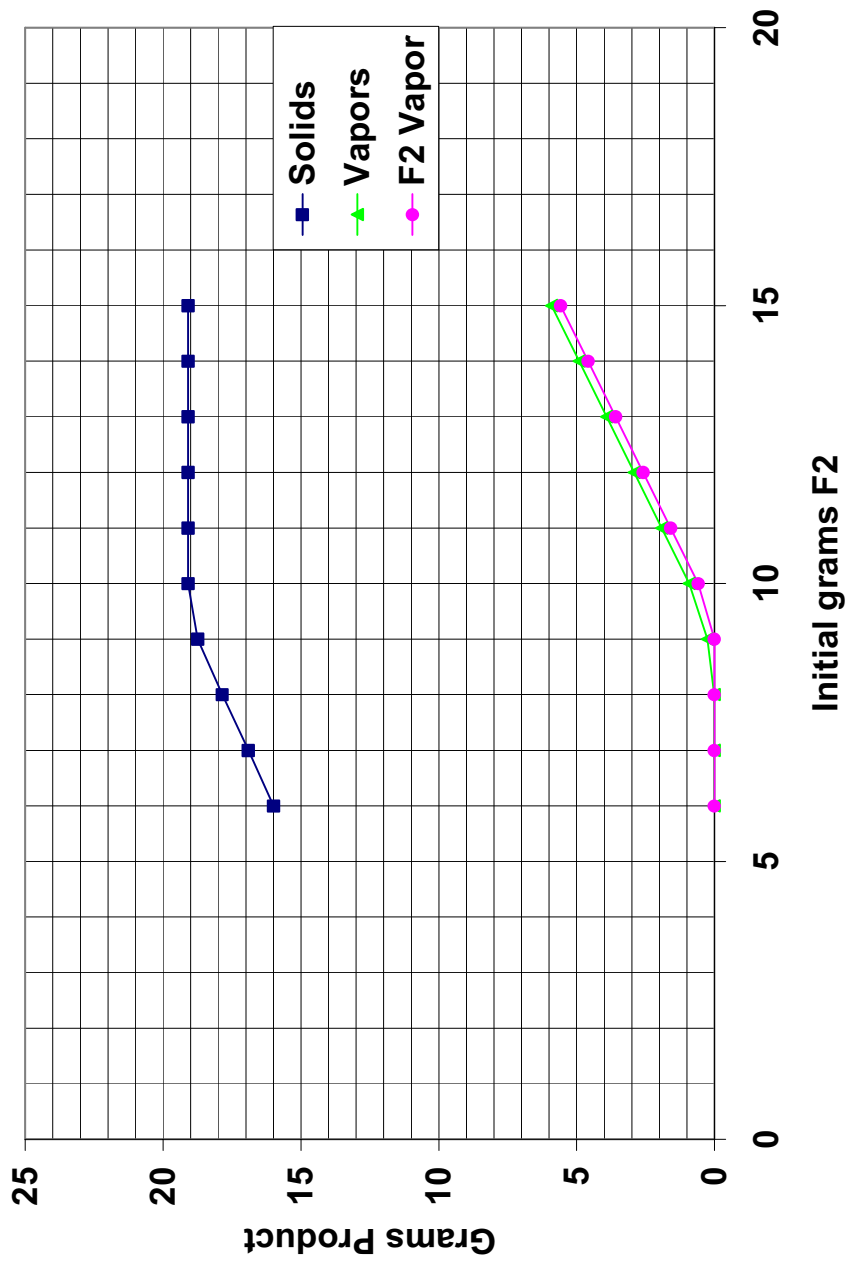


Figure C.3: Products from reaction of varying amounts of F₂ gas with 50.3% SS-316 and 49.7% Zircaloy-2, at 100 C

Initial Grams of Fluorine	P(atm)	g-F ₂ (g)	g-MoF ₆ (g)	g-CF ₄ (g)	g-SF ₆ (g)	g-PF ₅ (g)	g-SiF ₄ (g)
6.0	0.001	0.000	0.000	0.000	0.000	0.000	0.007
7.0	0.001	0.000	0.000	0.000	0.000	0.000	0.007
8.0	0.001	0.000	0.000	0.000	0.000	0.000	0.007
9.0	0.006	0.000	0.000	0.000	0.000	0.008	0.007
10.0	0.129	0.581	0.276	0.029	0.009	0.008	0.007
11.0	0.326	1.581	0.276	0.029	0.009	0.008	0.007
12.0	0.524	2.581	0.276	0.029	0.009	0.008	0.007
13.0	0.722	3.581	0.276	0.029	0.009	0.008	0.007
14.0	0.920	4.581	0.276	0.029	0.009	0.008	0.007
15.0	1.117	5.581	0.276	0.029	0.009	0.008	0.007

Table C.2: Pressure and major gaseous products from reaction of varying amounts of F₂ gas with 50.3% SS-316 and 49.7% Zircaloy-2, at 100 C

A study of varying temperatures of the fluorination of SS-316/Zircaloy2 mix shows temperatures between 20 – 100C produces an identical vapor composition. This is shown in Figure C.4. Note the similarity to Figure 5.3. Actual numbers are given in Table C.3.

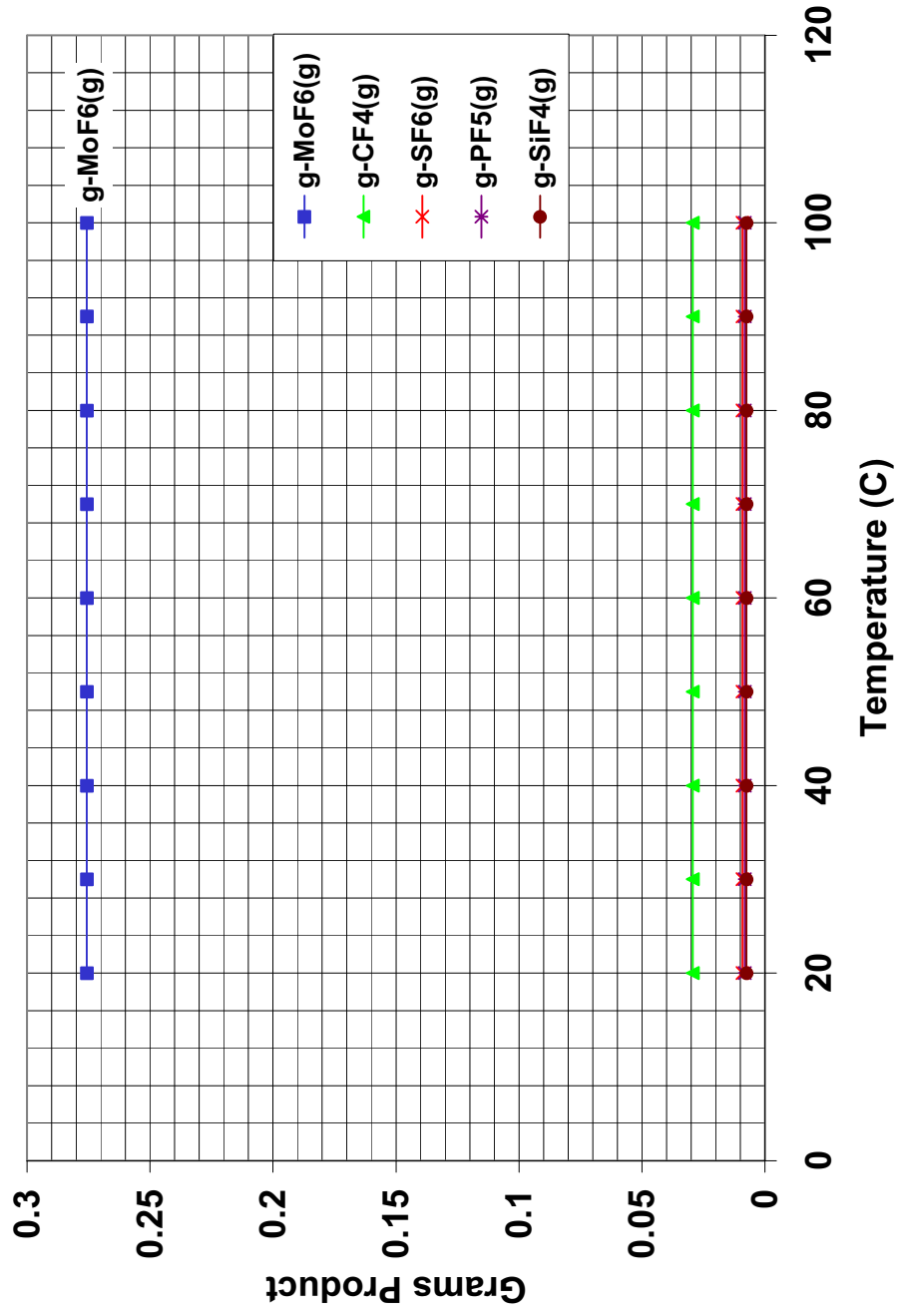


Figure C.4: Major gaseous products from reaction of 50.3% SS-316 & 49.7% Zircaloy-2 with 14.6g F₂ (20 - 100C)

Product	Grams of Vapor
g-MoF ₆ (g)	2.76E-01
g-CF ₄ (g)	2.93E-02
g-SF ₆ (g)	9.11E-03
g-PF ₅ (g)	8.13E-03
g-SiF ₄ (g)	7.41E-03

Table C.3: Major gaseous products from reaction of 50.3% SS-316 & 49.7% Zircaloy-2 with 14.6g F₂ (100C)

A model of varying amount of initial feed metal with the same 14.6 g initial F₂ was run as well. The results are shown in Figure C.5. The results are as expected. More than 16 grams of feed consumes all of the F₂. Above 16 g feed, the F₂ selectively reacts to create solid fluorides with the exception of SiF₄. A 10 gram initial feed metal sample is adequate for this experiment.

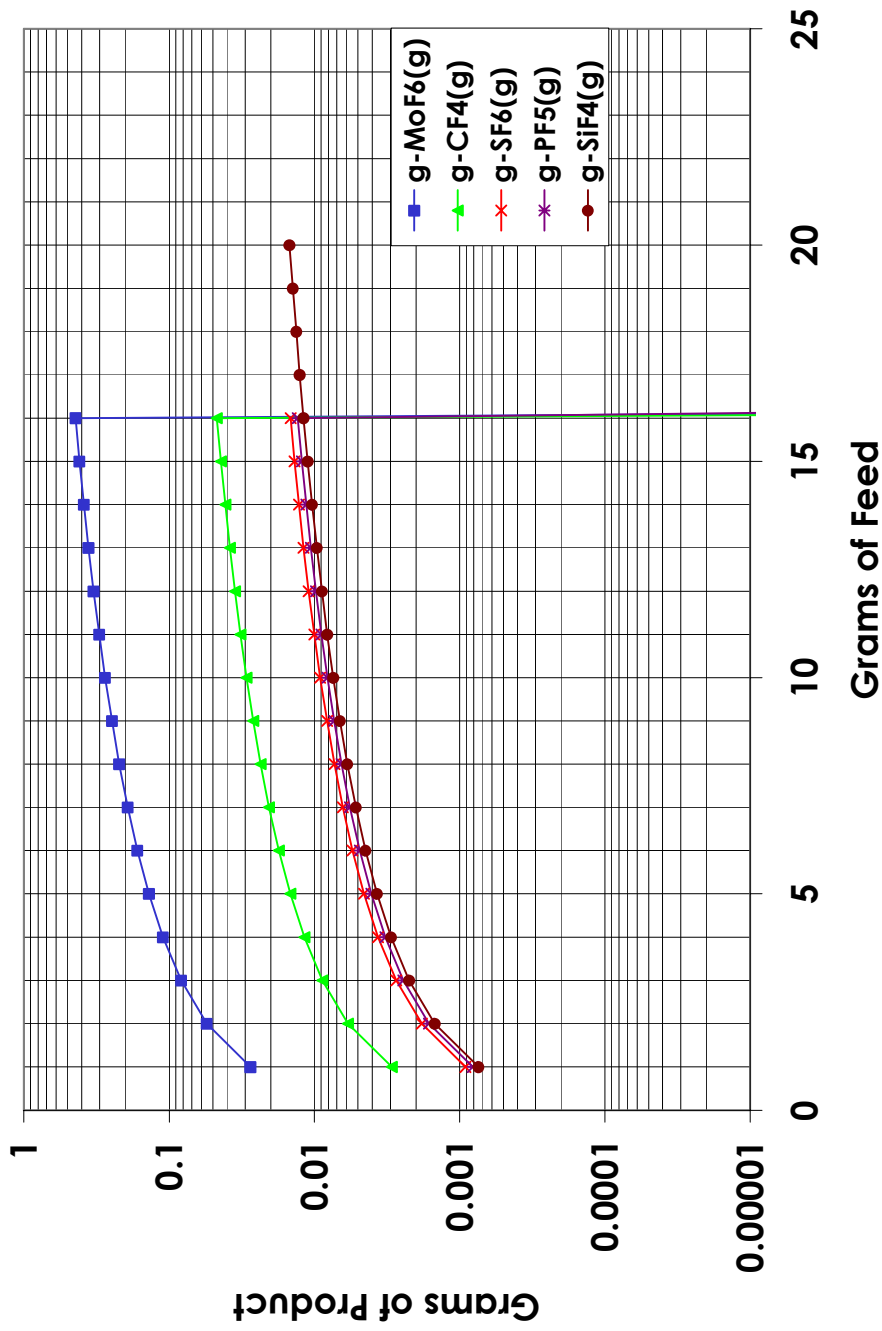


Figure C.5: Major gaseous products from reaction of 50.3% SS-316 & 49.7% Zircaloy-2 with 14.6g F₂ (20 – 100 C)

Modeling oxygen contamination was the next concern. Initially a model of O₂ interacting with the feed metal (along with F₂) was modeled. In the experiment described, it would actually be air getting into the vessel that would be a concern. This means 79% N₂ and 21% O₂. It seems proper that any air that entered the vessel would probably displace an equal mass of F₂. Cases were also run where F₂ was not displaced. Results for both trials were similar. As expected, more products are predicted with the presence of air (Figures C.6 and C.7). The majority of the new products are compounds of fluorine, nitrogen and oxygen. A large proportion of NF₃ is produced, along with a few other N-O-F compounds. NF₃ (bp = -129C) should not condense to any great extent, and shouldn't be a concern. All of the F₂ is consumed when more than 1.25 grams of air are introduced into the system. There are also undoubtedly some compounds that are unaccounted for in the analysis. For these reasons, air contamination should be kept to a minimum.

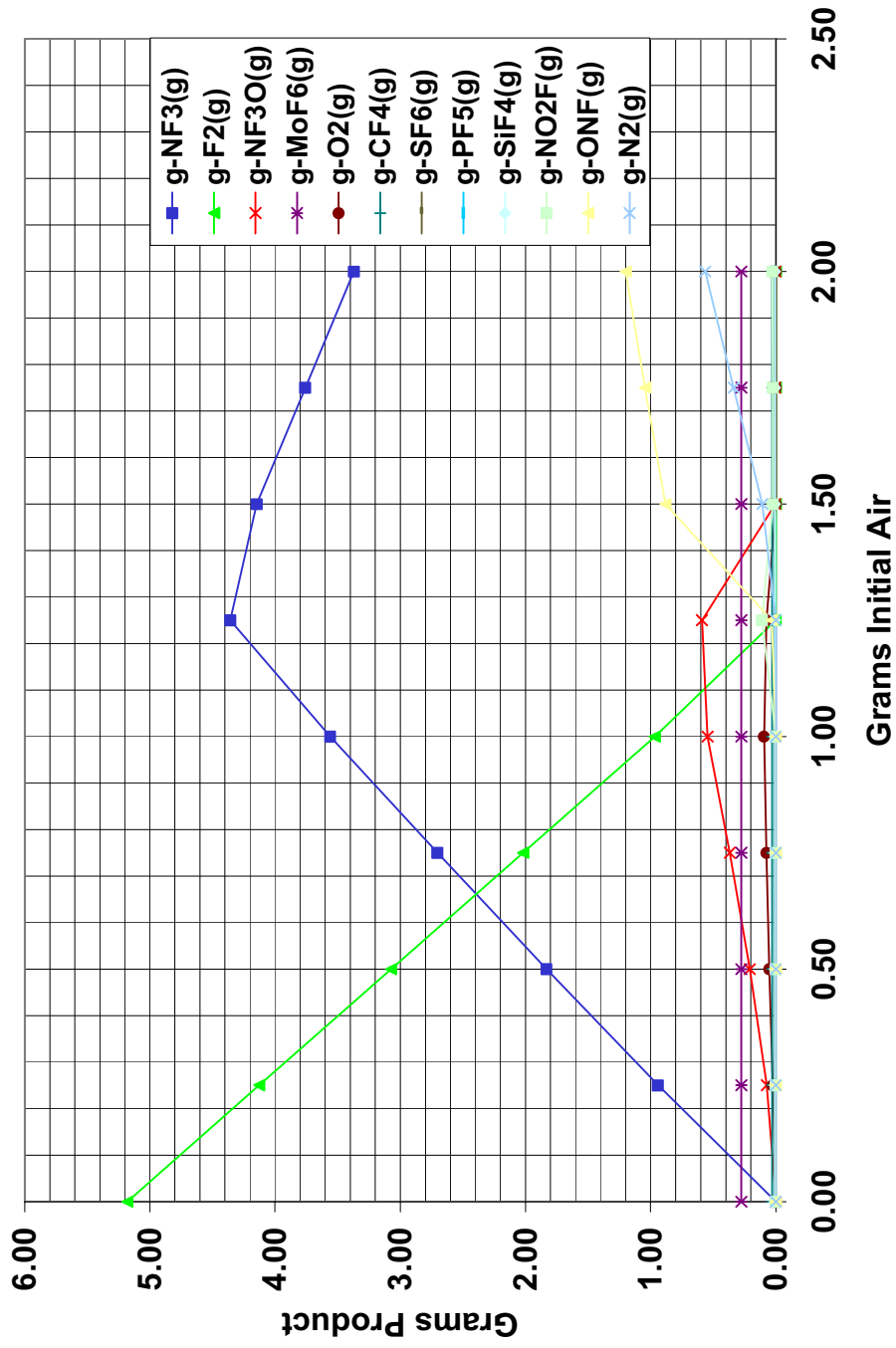


Figure C.6: Gaseous products from reaction of F₂ gas with SS-316/Zircaloy2, with varying amounts of initial air/F₂ mix

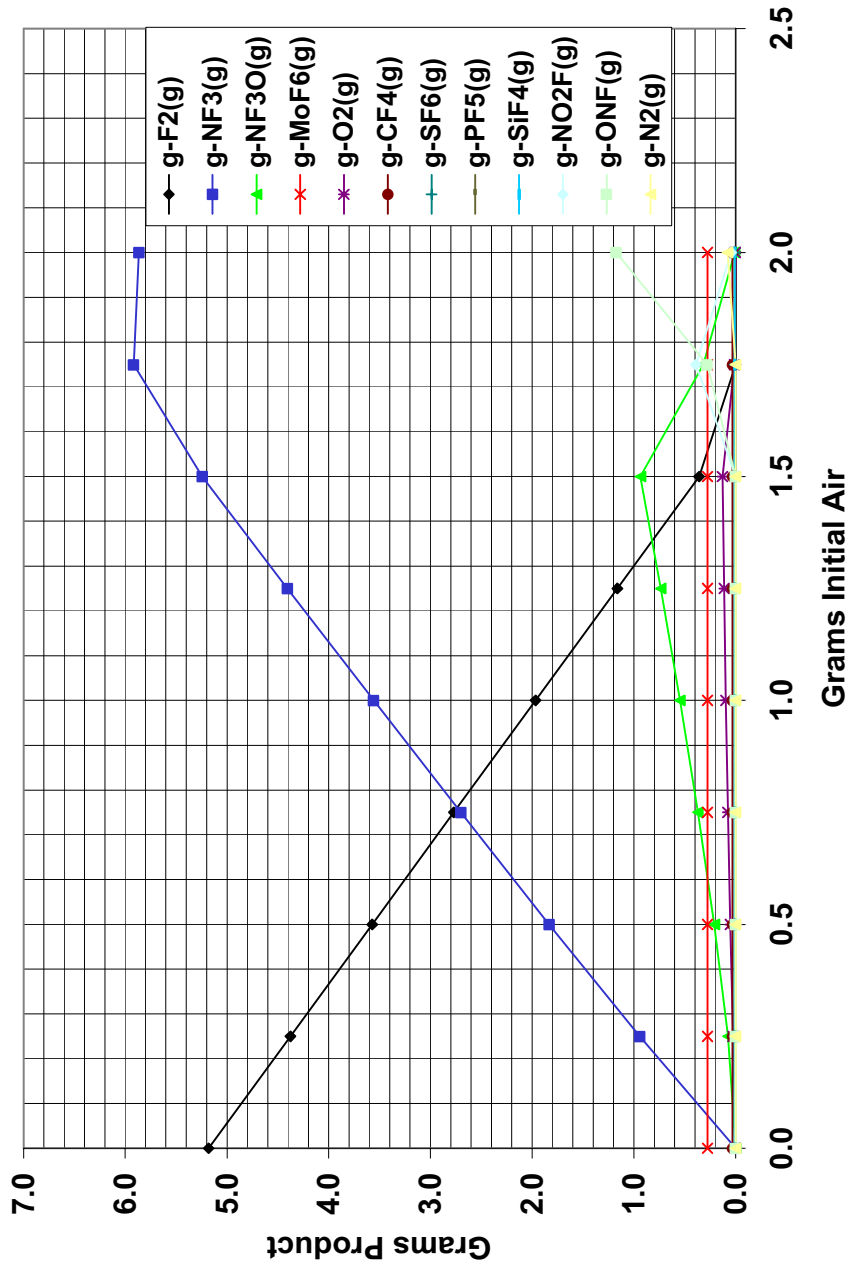


Figure C.7: Gaseous products from reaction of F₂ gas with SS-316/Zircaloy2, with varying amounts of initial air (constant F₂)

Grams Initial Air	0.000	0.250	0.500	0.750	1.000	1.250	1.500	1.750	2.000
g-ZrF ₄ (s)	8.938	8.938	8.938	8.938	8.938	8.938	8.938	8.938	8.938
g-FeF ₃ (s)	6.751	6.751	6.751	6.751	6.751	6.751	6.751	6.751	6.751
g-NF ₃ (g)	0.000	0.941	1.832	2.702	3.559	4.357	4.147	3.758	3.371
g-CrF ₄ (s)	2.117	2.117	2.117	2.117	2.117	2.117	2.117	2.117	2.117
g-F ₂ (g)	5.181	4.127	3.073	2.020	0.966	0.001	0.000	0.000	0.000
g-NiF ₂ (s)	0.998	0.998	0.998	0.998	0.998	0.998	0.998	0.998	0.998
g-NF ₃ O(g)	0.000	0.074	0.208	0.369	0.546	0.592	0.004	0.003	0.003
g-MoF ₆ (g)	0.276	0.276	0.276	0.276	0.276	0.276	0.276	0.276	0.276
g-MnF ₃ (s)	0.206	0.206	0.206	0.206	0.206	0.206	0.206	0.206	0.206
g-SnO ₂ (s)	0.028	0.095	0.095	0.095	0.095	0.095	0.095	0.095	0.095
g-O ₂ (g)	0.000	0.025	0.052	0.075	0.095	0.075	0.000	0.000	0.000
g-CF ₄ (g)	0.029	0.029	0.029	0.029	0.029	0.029	0.029	0.029	0.029
g-SF ₆ (g)	0.009	0.009	0.009	0.009	0.009	0.009	0.009	0.009	0.009
g-PF ₅ (g)	0.008	0.008	0.008	0.008	0.008	0.008	0.008	0.008	0.008
g-SiF ₄ (g)	0.007	0.007	0.007	0.007	0.007	0.007	0.007	0.007	0.007
g-NO ₂ F(g)	0.000	0.000	0.000	0.000	0.000	0.111	0.024	0.024	0.028
g-ONF(g)	0.000	0.000	0.000	0.000	0.000	0.031	0.883	1.044	1.200

Table C.4: Gaseous products from reaction of F₂ gas with SS-316/Zircaloy2, with varying amounts of initial air/F₂

Grams Initial Air	0.000	0.250	0.500	0.750	1.000	1.250	1.500	1.750	2.000
g-ZrF ₄ (s)	8.938	8.938	8.938	8.938	8.938	8.938	8.938	8.938	8.938
g-FeF ₃ (s)	6.751	6.751	6.751	6.751	6.751	6.751	6.751	6.751	6.751
g-F ₂ (g)	5.181	4.377	3.573	2.770	1.966	1.163	0.359	0.000	0.000
g-NF ₃ (g)	0.000	0.941	1.832	2.702	3.559	4.405	5.244	5.919	5.865
g-CrF ₄ (s)	2.117	2.117	2.117	2.117	2.117	2.117	2.117	2.117	2.117
g-NiF ₂ (s)	0.998	0.998	0.998	0.998	0.998	0.998	0.998	0.998	0.998
g-NF ₃ O(g)	0.000	0.074	0.208	0.369	0.546	0.735	0.934	0.316	0.008
g-MoF ₆ (g)	0.276	0.276	0.276	0.276	0.276	0.276	0.276	0.276	0.276
g-MnF ₃ (s)	0.206	0.206	0.206	0.206	0.206	0.206	0.206	0.206	0.206
g-SnO ₂ (s)	0.028	0.095	0.095	0.095	0.095	0.095	0.095	0.095	0.095
g-O ₂ (g)	0.000	0.025	0.052	0.075	0.095	0.113	0.129	0.012	0.000
g-CF ₄ (g)	0.029	0.029	0.029	0.029	0.029	0.029	0.029	0.029	0.029
g-SF ₆ (g)	0.009	0.009	0.009	0.009	0.009	0.009	0.009	0.009	0.009
g-PF ₅ (g)	0.008	0.008	0.008	0.008	0.008	0.008	0.008	0.008	0.008
g-SiF ₄ (g)	0.007	0.007	0.007	0.007	0.007	0.007	0.007	0.007	0.007
g-NO ₂ F(g)	0.000	0.000	0.000	0.000	0.000	0.000	0.001	0.391	0.043
g-ONF(g)	0.000	0.000	0.000	0.000	0.000	0.000	0.000	0.279	1.174

Table C.5: Gaseous products from reaction of F₂ gas with SS-316/Zircaloy2, with varying amounts of initial air (constant F₂)

Figures C.6 and C.7 (and Tables C.4 and C.5) show that the final metal halide products are the same as those listed in Table 5.1. This prediction is probably a kinetics issue. Equilibrium models like FACTSage® predict the most stable compounds of a system. Fluoride compounds are nearly always the most stable compounds, however it might take a great deal of time to fully fluorinate the oxides. This time is not predicted by FACTSage®, and should be noted. Performing the proposed experiment will help determine the effect of kinetics on this fluorination scheme.

C.3 Review of Surrogate Experiment Modeling

Modeling predicts full fluorination and volatilization of Mo to MoF₆. The results agree with the results from AFCI fuel modeling in that MoF₆ (the surrogate for TcF₆), along with a few other fluorides, are the only volatile compounds generated. This experiment is fairly easy to perform and could be done at minimal cost. The experimental results would also help support or refute the concept of the fluoride volatility process. The greatest uncertainty with this approach is the lack of sufficient thermochemical and kinetic data to properly model the fluorination step. This experiment will help determine the effect of kinetics on the reaction. This could also produce some of the products that FACTSage® does not have in its database. These can be analyzed and studied for inclusion in the model. This surrogate experiment will also help predict problems that might occur with the fluorination of the AFCI fuel.